Striatal pathways in dyskinesia and dystonia

Andreoli, Laura

2021

Document Version:
Publisher's PDF, also known as Version of record

Striatal pathways in dyskinesia and dystonia

LAURA ANDREOLI | FACULTY OF MEDICINE | LUND UNIVERSITY

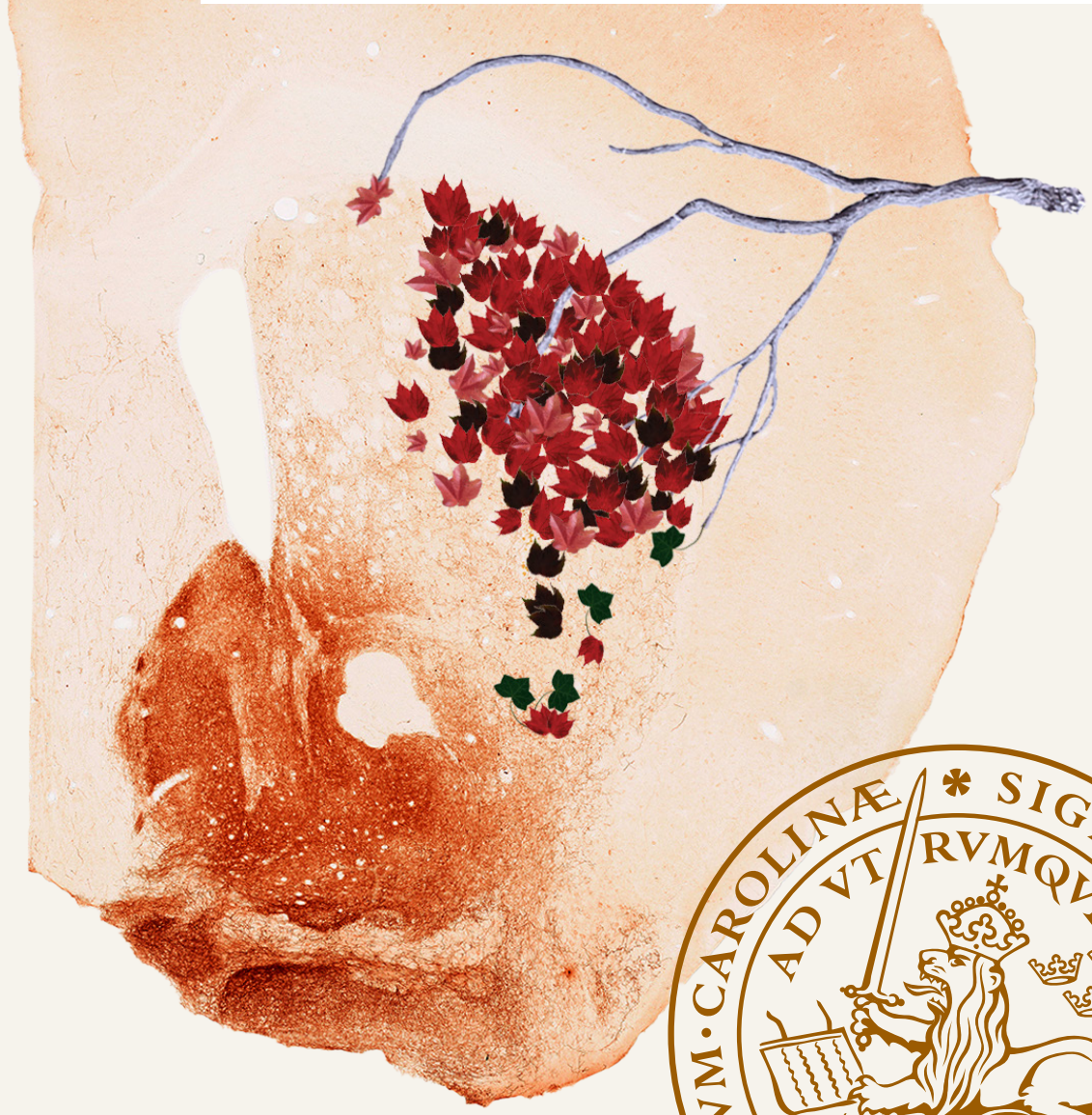

Printed by Media-Tryck, Lund 2021 NORDIC SWAN ECOLABEL 3041 0903

LUND UNIVERSITY

FACULTY OF MEDICINE

Department of Experimental Medical Science

Lund University, Faculty of Medicine
Doctoral Dissertation Series 2021:146
ISBN 978-91-8021-153-6
ISSN 1652-8220

Striatal pathways in dyskinesia and dystonia

Laura Andreoli

LUND
UNIVERSITY

DOCTORAL DISSERTATION

by due permission of the Faculty of Medicine, Lund University, Sweden.
This thesis will be defended on December 14th, 2021, in Segerfalksalen,
Wallenberg Neuroscience Center, Lund, Sweden.

Faculty opponent
Prof. Rosario Moratalla
Cajal Institute, Consejo Superior de Investigationes Cientificas (CSIC)
Avenida Dr. Arce, 37, 28002, Madrid, Spain

Organization LUND UNIVERSITY	**Document name** Doctoral Dissertation
	Date of issue 14th of December 2021
Author(s) **Laura Andreoli**	Sponsoring organization

Title and subtitle
Striatal pathways in dyskinesia and dystonia

Abstract

Purposeful and well-coordinated movements depend on the control exerted by dopamine (DA) on the basal ganglia (BG) network. Accordingly, dysfunctions or lesions of the dopaminergic system in the BG can result in an overall poverty and slowness of movement, cardinal features of Parkinson´s disease (PD), or in dyskinesias, exaggerated and involuntary movements resulting from L-DOPA pharmacotherapy.

The corpus striatum is the fulcrum of DA-dependent movement control. From this structure originate two pathways that are thought to modulate movement in opposite ways. The movement-promoting pathway ('direct pathway') originates from striatal projection neurons (dSPNs) expressing dopamine (DA) D1 receptors (D1Rs), whereas the movement-suppressing pathway ('indirect pathway') originates from striatal neurons (iSPNs) expressing D2 receptors (D2R).

Classic theories attribute L-DOPA-induced dyskinesia (LID) to the overactivity of the movement-promoting pathway resulting from an aberrant activation of dSPN-D1R-mediated signalling in the DA-denervated striatum. However, these theories are inadequate to explain the complexity of LID, which cannot simply be equated with "more movement", but instead consists of a mixture of fast hyperkinetic motions and dystonic postures in varying combinations. The overarching aim of this thesis is to parse the involvement of striatal output pathways and DA receptor subtypes in treatment-induced dyskinesia and dystonia using rodent models of clinically manifest PD.

Using pathway-specific chemogenetic modulation, we demonstrate that selective iSPN stimulation promotes hypokinesia and inhibits the dyskinetic action of L-DOPA, while dSPN stimulation has opposite effects. Moreover, we prove that dSPN stimulation alone can induce mild dyskinesia, though not the full spectrum and severity of LID. In a second study, we show that D1Rs and metabotropic glutamate receptors type 5 form heteromers in the DA-denervated striatum, and that these receptor interactions are causally linked with dyskinesias mediated by D1R stimulation. Next, using a set of pharmacological tools and models of gene receptor ablation we show that D1R and D2R stimulation mediate different forms of dyskinesia. Specifically, D1R activation elicits mainly the hyperkinetic components of LID, whereas the D2R mediate mainly its dystonic features.

Taken together, the results of this thesis present a refinement of the pathophysiological notions regarding the contribution of striatal pathways to the motor features of PD and LID, paving the way for more effective treatment options.

Key words
Striatum, Parkinson´s diseas, L-DOPA-induced dyskinesia, dystonia, mouse model, DREADDs

Classification system and/or index terms (if any)

Supplementary bibliographical information	**Language** English
ISSN and key title 1652-8220	**ISBN** 978-91-8021-153-6
Recipient's notes	**Number of pages** 99 / Price
	Security classification

Signature Laura Andreoli Date 2021-11-01

Striatal pathways in dyskinesia and dystonia

LUND
UNIVERSITY

Coverphoto by Laura Andreoli: "*Unilateral striatal models in Lund: fall season.*"

Faculty of Medicine
Department of Experimental Medical Science

ISBN 978-91-8021-153-6
ISSN 1652-8220

Printed in Sweden by Media-Tryck, Lund University
Lund 2021

Ai miei Nonni

Table of Contents

Papers and Manuscript

I. Chemogenetic stimulation of striatal projection neurons modulates responses to Parkinson´s disease therapy

Alcacer C, Andreoli L, Sebastianutto I, Jakobsson J, Fieblinger T, Cenci MA

J Clin Invest 2017; 127(2):720-734

II. D1-mGlu5 heteromers mediate noncanonical dopamine signaling in Parkinson's disease

Sebastianutto I, Goyet E, Andreoli L*, Font-Ingles J*, Moreno-Delgado D, Bouquier N, Jahannault-Talignani C, Moutin E, Di Menna L, Maslava N, Pin JP, Fagni L, Nicoletti F, Ango F, Cenci MA§, Perroy J§

J Clin Invest 2020; 130(3):1168-84

III. Distinct patterns of dyskinetic and dystonic features following D1 or D2 receptor stimulation in a mouse model of parkinsonism

Andreoli L, Abbaszadeh M, Cao X, Cenci MA

Neurobiol Dis 2021; 157:105429

IV. Pivotal role of indirect pathway-D2 receptors in parkinsonian and dyskinetic states

Andreoli L, Alcacer C, Jakobsson J, Cenci MA

Manuscript

Summary

Purposeful and well-coordinated movements depend on the control exerted by dopamine (DA) on the basal ganglia (BG) network. Accordingly, dysfunctions or lesions of the dopaminergic system in the BG can either result in poverty and slowness of movement, cardinal features of Parkinson´s disease (PD), or in dyskinesias, exaggerated and involuntary movements resulting from L-DOPA pharmacotherapy.

The corpus striatum is the fulcrum of DA-dependent movement control. From this structure originate two pathways that are thought to modulate movement in opposite ways. The movement-promoting pathway ('direct pathway') originates from striatal projection neurons (dSPNs) expressing dopamine (DA) D1 receptors (D1Rs), whereas the movement-suppressing pathway ('indirect pathway') originates from striatal neurons (iSPNs) expressing D2 receptors (D2R).

Classic theories attribute L-DOPA-induced dyskinesia (LID) to the overactivity of the movement-promoting pathway resulting from an aberrant activation of dSPN-D1R-mediated signalling in the DA-denervated striatum. However, these theories are inadequate to explain the complexity of LID, which cannot simply be equated with "more movement", but instead consists of a mixture of fast hyperkinetic motions and dystonic postures in varying combinations. The overarching aim of this thesis is to parse the involvement of striatal output pathways and DA receptor subtypes in treatment-induced dyskinesia and dystonia using rodent models of clinically manifest PD.

Using pathway-specific chemogenetic modulation, we demonstrate that selective iSPN stimulation promotes hypokinesia and inhibits the dyskinetic action of L-DOPA, while dSPN stimulation has opposite effects. Moreover, we prove that dSPN stimulation alone can induce mild dyskinesia, though not the full spectrum and severity of LID. In a second study, we show that D1Rs and metabotropic glutamate receptors type 5 form heteromers in the DA-denervated striatum, and that these receptor interactions are causally linked with dyskinesias mediated by D1R stimulation. Next, using a set of pharmacological tools and models of receptor gene ablation, we show that D1R and D2R stimulation mediate different forms of dyskinesia. Specifically, D1R activation elicits mainly the hyperkinetic components of LID, whereas the D2R mediate mainly its dystonic features.

Taken together, the results of this thesis present a refinement of pathophysiological notions regarding the contribution of striatal pathways to the motor features of PD and LID, paving the way for more effective treatment options.

Populärvetenskaplig sammanfattning

Utförandet av ändamålsenliga och välkoordinerade rörelser är beroende av signalsubstansen dopamin (DA) som reglerar nervcellsaktivitet i hjärnans basala ganglier. Förändringar inom det dopaminerga systemet kan därför orsaka generellt försämrad rörelseförmåga med långsamma rörelser (klassiska tecken på Parkinsons sjukdom; PS), men även kraftiga och ofrivilliga rörelser, s.k. dyskinesier. De senare är en vanlig komplikation vid L-DOPA behandling av PS (då känt som L-DOPA inducerade dyskinesier; LID).

Det är främst inom basala gangliernas största kärna, striatum, som DA utövar sina effekter på rörelsekontroll. Från denna struktur sträcker sig två signalvägar som tros påverka rörelser på motsatta sätt, och som uttrycker olika mottagarprotein (’receptorer’) för DA på sitt cellmembran. Den ena signalvägen (den direkta banan) anses vara rörelseinducerande och har sitt ursprung i striatala nervceller (dSPNs) som uttrycker dopamin D1 receptorer (D1R). Den andra signalvägen (den indirekta banan) anses vara rörelsehämmande och har sitt ursprung i striatala nervceller (iSPNs) som uttrycker dopamin D2 receptorer (D2R). Klassiska modeller av LID är baserade på idén att L-DOPA behandling orsakar en överaktivitet i den direkta banans D1R-bärande dSPN celler. Dessa modeller ger dock inte tillfredställande förklaringar av LIDs komplexitet, vilken inte bara kan beskrivas som "mer rörelser", utan snarare består av en blandning av snabba hyperkinetiska rörelser samt långsamma och krampaktiga kroppshållningar (dystonier).

Det övergripande målet för denna avhandling är att klarlägga rollerna som olika striatala signalvägar och deras tillhörande DA receptorer har i behandlingsinducerad dyskinesi och dystoni i gnagarmodeller av kliniskt manifesterad PS. Genom att använda signalvägsspecifik kemogenetisk modulering visar vi att selektiv stimulering av den indirekta banans iSPNs främjar hypokinesi och inhiberar LID, medan stimulering av den direkta banans dSPNs har motsatt effekt. Vidare visar vi att stimulering av endast dSPNs inducerar en mild dyskinesi, som är mindre allvarlig än LID och inte täcker samma spektrum av rörelsestörningar. I en annan studie visar vi att D1Rs interagerar med en viss typ av glutamatreceptor (mGlu5) i det DA-svultna striatum, och att denna interaktion förmedlar onormala cellsignaler som är kopplade till LID. Slutligen visar vi att stimulering av D1R och D2R medierar olika former av dyskinesi. Aktivering av D1R framkallar huvudsakligen LIDs hyperkinetiska komponenter medan D2R huvudsakligen styr dess dystona drag.

Tillsammans ger resultaten i dessa studier en förbättrad bild av de patofysiologiska mekanismerna bakom olika striatala signalvägars roll i de motoriska dragen i PS och LID, vilket i sin tur öppnar upp möjligheter för att framgent utveckla bättre behandlingar.

Riassunto

Movimenti precisi e coordinati del nostro corpo dipendono dal controllo esercitato dalla dopamina sul circuito dei gangli della base. Disfunzioni o danni del sistema dopaminergico possono manifestarsi sia come riduzione generale e lentezza nei movimenti, che come ritmiche e involontarie fluttuazioni motorie. I primi sono sintomi caratteristici della malattia di Parkinson, mentre i secondi sono meglio conosciuti come discinesie. Queste ultime, si manifestano dopo una prolungata assunzione di L-DOPA, precursore della dopamina e principale trattamento farmacologico nel Parkinson.

Il corpo striato, appartenente al circuito dei gangli della base, svolge una funzione essenziale nel controllo motorio. Dai neuroni dello striato originano due vie efferenti che sembrerebbero controllare il movimento in modalità opposte. La via diretta, considerata “promotrice” del movimento, è composta dagli assoni dei neuroni striatali che esprimono i recettori dopaminergici di tipo D1. contrariamente, la via indiretta che ha la proprietà di inibire il movimento, è caratterizzata dalla presenza di recettori per la dopamine di tipo D2.

Classicamente, le discinesie indotte da L-DOPA vengono imputate all’iperattività della via diretta conseguente ad un’ eccessiva stimolazione dei recettori D1. Tuttavia, questa teoria risulta inadeguata a spiegare la complessità che caratterizza questi movimenti. Le discinesie, infatti, non possono essere semplicemente equiparate a "più movimento", ma consistono in una combinazione di movimenti veloci, ipercinetici e di posture lente e di natura distonica.

L'obiettivo generale di questa tesi è perciò quello di chiarire il contributo delle due vie striatali e dei recettori D1 e D2 nelle discinesie e nelle distonie indotte da L-DOPA, utilizzando modelli murini di Parkinson.

Nel primo studio, dimostriamo che la stimolazione chemogenetica dei neuroni striatali della via indiretta causa ipocinesia e riduzione dell’ azione discinetica della L-DOPA, mentre effetti opposti si osservano dalla stimolazione dei neuroni della via diretta. Inoltre, l’attivazione chemogenetica selettiva dei neuroni della via diretta è di per sé sufficiente a produrre movimenti discinetici, anche in assenza di L-DOPA, sebbene di severità più moderata. Nel secondo studio, mostriamo che in assenza di dopamina i recettori D1 e quelli per il glutammato di tipo mGlu5 interagiscono fra loro formando eteromeri, attivando così meccanismi intracellulari che favoriscono lo sviluppo delle discinesie. Successivamente, nel terzo e quarto studio, combinando il classico approccio farmacologico a manipolazioni genetiche in-vivo, mostriamo come la mirata stimolazione dei recettori D1 e D2 moduli le diverse forme di discinesie. Nello specifico, l'attivazione dei recettori D1 stimola principalmente lo sviluppo di

componenti ipercinetiche, mentre la stimolazione dei recettori D2 è responsabile primariamente della compenete distonica.

List of abbreviations

6-OHDA	6-hydroxy-dopamine
A2aR	adenosine a2a receptor
AAV	adeno-associated virus
AC	adenylyl cyclase
AIMs	abnormal involuntary movements
AMPAR	amino-3-hydroxy-5-methyl-4-isoxazolepropionic acid receptor
AP	antero-posterior
BAC	bacterial artificial chromosome
BBB	blood brain barrier
BG	basal ganglia
Ca^{2+}	calcium
cAMP	cyclic adenosine monophosphate
CIN	cholinergic interneuron
CNO	clozapine n-oxide
Cre	cre recombinase
D1R	dopamine D1 receptor
D2R	dopamine D2 receptor
D3R	dopamine D3 receptor
D4R	dopamine D4 receptor
D5R	dopamine D5 receptor
DA	dopamine
DAR	dopamine receptors
DARPP-32	dopamine and camp-regulated phosphoprotein 32
DBS	deep-brain-stimulation
DREADD	designer receptor exclusively regulated by designer drugs
dSPN	direct pathway spiny projection neuron
DV	dorso-ventral
ERK1/2	extracellular signal regulated kinase 1 and 2
GABA	aminobutiric acid
GPCR	G-protein coupled receptors
GP	globus pallidus
GPe	globus pallidus pars externa
GPi	globus pallidus pars interna

IHC	immunohistochemistry
InsP	inositol monophosphate
IP3	inositol triphosphate
iSPN	indirect pathway spiny projection neurons
KD	knock-down
KO	knock-out
L-DOPA	L-3,4 dihydroxyphenylalanine
LID	L-DOPA-induced dyskinesia
M1	muscarinic receptor type 1
M3	muscarinic receptor type 3
M4	muscarinic receptor type 4
MAPK	mitogen-activated protein kinases
MFB	medial forebrain bundle
mGluR5	metabotropic glutamate receptor type 5
ML	medio-lateral
MPTP	1-methyl-4- phenyl-1,2,3,6-tetrahydropyridine
NMDAR	N-methyl-d-aspartate receptor
PFA	paraformaldehyde
PI	phosphoinositide
PD	parkinson´s disease
PKA	protein kinase A
PKC	protein kinase C
PLC	phospholipase C
PPA	preproenkephalin-A
Ser	serine
SNc	substantia nigra pars compacta
SNr	substantia nigra pars reticulata
SPN	spiny projection neurons
STN	subthalamic nucleus
TH	tyrosine hydroxylase
Thr	threonine
Tyr	tyrosine
VTA	ventral tegmental area
WT	wild type

Introduction

Introduction

The basal ganglia

The basal ganglia (BG) are a group of densely interconnected nuclei located between the base of the forebrain and the midbrain. Anatomically, the term BG is restricted to five subcortical structures: the striatum, the globus pallidus (GP; pars interna, GPi and pars esterna, GPe) the subthalamic nucleus (STN) and the subtantia nigra (SN; pars reticulata, SNr, and pars compacta, SNc). Together with the cortex, the thalamus and the brain stem, the BG nuclei form the "motor circuit", a network that controls execution and selection of movements and voluntary actions (Albin et al., 1989; Nelson and Kreitzer, 2014; Redgrave et al., 1999); where the striatum is the main receiving input, whereas the GPi and SNr are the output nuclei of the BG, sending signals to the rest of the brain.

Not only is the striatum the largest nucleus of the BG but it also represents the most densely innervated structure by cortical afferents. Indeed, the striatum receives glutamatergic excitatory inputs from nearly all cortical areas (Redgrave et al., 2010) and from the thalamus (intralaminar nuclei, centromedian and parafascicular complex, mediodorsal and ventrolateral nuclei) (Smith et al., 2004) alongside with dopaminergic projections from the SNc and the ventral tegmental area (VTA) (Smith and Kieval, 2000). In primates, the striatum is composed of two segments separated by the condensed fibers of the internal capsule (the caudate nucleus and the putamen), while in the rodents appears as a single structure.

Approximately 95% of the striatal neurons are identified as spiny projection neurons (SPNs) (Tepper et al., 2004); gamma-amynobutyric acid (GABA)-releasing neurons defined by a medium-size soma (10-20 μm diameter) and numerous dendritic spines (Kawaguchi, 1997). Based on their projection´s targets and their histological properties, SPNs are segregated into two different subpopulations that give rise to two major pathways of the BG circuitry. One population, the so-called striatonigral SPNs, projects directly to the main output nuclei SNr and GPi and form the "direct pathway". Direct pathway SPNs (dSPNs) are mainly identified for expressing the peptides dynorphin and substance P (Beckstead and Kersey, 1985; Chesselet and Graybiel, 1983; Gerfen et al., 1991), the muscarinic receptor M4 (Bernard et al., 1992; Hersch et al., 1994) and the dopamine (DA) receptor D1 (D1R) (Gerfen et al., 1990). The second population, the striatopallidal SPNs, projects instead indirectly to the output nuclei via an intermediate connection to the GPe and give rise to the so called "indirect pathway". Spiny neurons of the indirect pathway (iSPNs) are distinguished from

their counterparts dSPNs for expressing the neuropeptide enkephalin, the adenosine A2a receptor (A2aR) and the DA receptor D2 (D2R) (Gerfen et al., 1990).

The remaining 5% of striatal neurons are "aspiny" interneurons and form dense microcircuitries within the striatum (Fino et al., 2018; Gittis and Kreitzer, 2012). Acetylcholine transferase (ChAT) positive aspiny neurons, the so-called cholinergic interneurons (CINs), release acetylcholine and account for approximately 1% of the total striatal interneurons (Kawaguchi, 1993; Kawaguchi et al., 1995). Differently, the remaining 4% communicates via the release of the inhibitory transmitter GABA, producing a local source of inhibition to the targeted cells. Up to now, seven different populations of GABA-ergic interneuron have been identified and classified based on both their electrophysiological properties and molecular profile (Assous and Tepper, 2019; Munoz-Manchado et al., 2018).

Classical view of the BG circuitry

The classical "go/no-go" model proposed in 1989 by Albin and collaborators was based on the idea that movement control relied on the opposing modulation of the direct and indirect pathway over the output nuclei of the BG (Albin et al., 1989; Kravitz et al., 2010). According to this model, cortical and thalamic inputs converge to the striatum to be processed, and from here forwarded, directly or indirectly, to the BG output structures (GPi and SNr). Direct and indirect pathways exert an opposite effect on the output nuclei activity, inhibiting and activating GPi/SNr respectively. Neurons of GPi and SNr exert a tonic and strong inhibitory control over the motor thalamus, which in turn sends excitatory projections back to the motor cortex. Thus, activation of the direct pathway disinhibits the motor thalamus facilitating motor behaviour (go-pathway), while activation of the indirect pathway strengthens the output nuclei inhibition and consequently reduces the motor response (no-go-pathway) (see Figure 1).

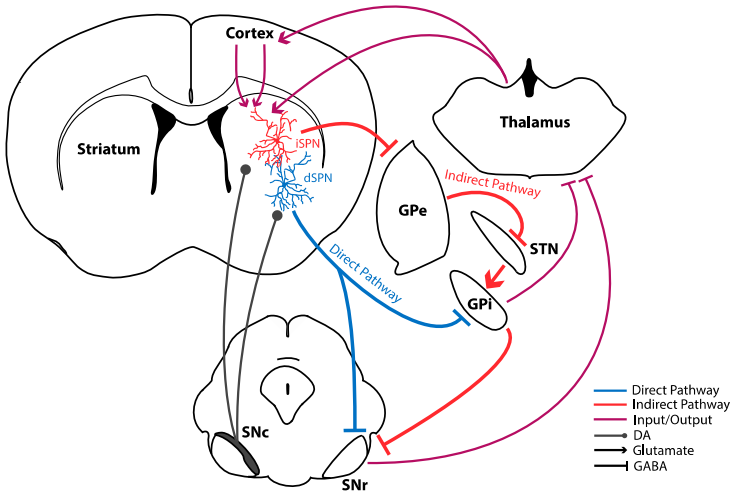

Figure 1: Representation of the classical organization of the BG circuitry in rodents. In blue, projections from striatal dSPNs form the direct pathway and target the output nuclei, GPi and SNr. Instead, highlighted in red, striatal iSPNs form the indirect pathway and project first to the intermediate structures GPe and SNT, and from there to the output nuclei. Projections from the GPi/SNr to the thalamus together with thalamo-cortical, thalamo-striatal and cortico-striatal projections are depicted in purple. Dopaminergic projectons are indicated in grey and originate from the SNc.

Novel view of the BG circuitry

More than 30 years after its debut, the classical "go/no-go model" still finds a large consensus in the scientific community. Yet, many other recent studies are challenging this view, adding interesting new insights to the classic functional organization of the BG circuitry.

One of these new models believes that rather working one opposite to each other, direct and indirect pathways work simultaneously to activate targeted movements and suppress unwanted ones. In this view, co-activation of the two major striatal pathways is necessary for a correct implementation of movement sequences and goal-directed behaviours (Cui et al., 2013; Klaus et al., 2017; Markowitz et al., 2018; Tecuapetla et al., 2014). Differently, another model believes that the function of iSPNs is not restricted to movement suppression, but these neurons can generate movement by allowing to switch between alternative motor programmes (Lee et al., 2021).

The necessity to revise the classical model finds additional support in new anatomical findings proving how the BG network follows a much more complex organization than the one that was originally proposed in Figure 1 (see Figure 2 for the updated view). For example, within the striatum SPNs form microcircuitries with other proximal SPNs through inhibitory axon collaterals (Dobbs et al., 2016; Lemos et al., 2016). Still in the striatum, neurochemically distinct pools of neurons are grouped together to form compartments namely the

matrix and the striosomes. These two compartments not only receive segregated inputs, but also project to different output structures, suggesting different physiological functionalities (Gerfen, 1984; Gerfen, 1985; Graybiel and Ragsdale, 1978). This novel complexity extends also to other structures of the BG network. The GPe for example, originally considered exclusive target of the indirect pathway, is currently known to also receive afferents from a small percentage of dSPNs collaterals (Cazorla et al., 2014). Still in the GPe, there are at least two main subpopulations of cells, the arkipallidal and prototypic neurons, with distinct electrophysiological and molecular properties, and distinct projection targets (Aristieta et al., 2021; Aristieta and Gittis, 2021; Mallet et al., 2012; Mallet et al., 2016; Mastro et al., 2014).

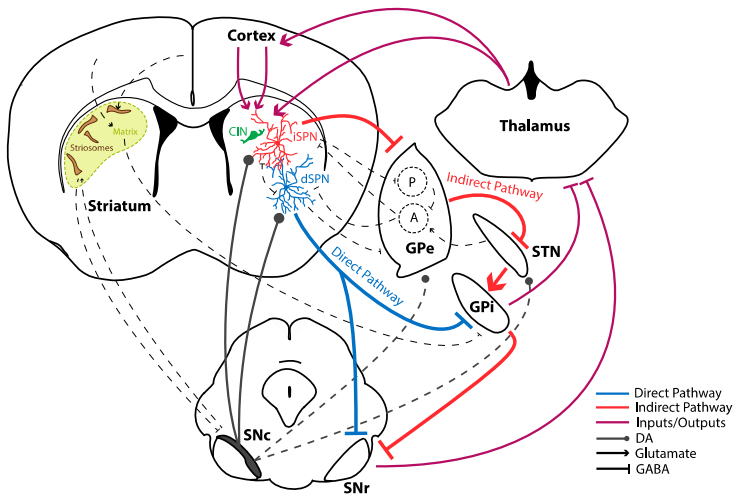

Figure 2: Updated view of the BG circuitry in rodents. New connections in the BG circuitry are depicted with black dashed lines. To mention some: 1) striosomes and matrix form anatomically distinct compartments within the striatum, receiving inputs from associative and limbic cortices and projecting to the SNc and to the GPi respectively; 2) dSPNs and iSPNs are connected to each other by bridging GABAergic collaterals; 3) CINs release acethylcoline in the striatum and modulate iSPNs and dSPNs activity; 4) arckipallidal (A) and prototypic (P) neurons in the GPe are distinct neuronal populations with different inputs and outputs; 5) SNc sends dopaminergic projection to the intermediate structures of the indirect pathway GPe and STN.

Dopamine and the dopamine receptors

DA constitutes the majority of the catecholamines content in the brain and represents an essential neurotransmitter of the central nervous system as it serves in the control of several vital functions such as movement, reward, sleep, attention, feeding and learning (Bjorklund and Dunnett, 2007). The direct precursor of DA is L-DOPA (l-3,4-dihydroxyphenylalanine), which is synthetized from tyrosine, and unlike DA has a large blood brain barrier (BBB) permeability. Like the other

catecholamines (norepinephrine, epinephrine), DA exerts its action by binding to five major types of receptors (numbered from 1 to 5) which are metabotropic receptors particularly abundant in the BG circuitry (Klein et al., 2019). The largest source of DA originates from midbrain neurons located in the SNc and VTA, whose projections reach several brain regions, including the striatum (Smith and Kieval, 2000). In the striatum, DA modulates cells excitability and synaptic functions by interacting with a heterogeneous pool of five different DA receptors (DARs). All five DARs (D1R, D2R, D3R, D4R and D5R) share the same seven-transmembrane structure, and function via G-protein mediated signalling (G-protein coupled receptor, GPCRs) to regulate adenylyl cyclase (AC) activity, cAMP production and phosphorylation of downstream targets (Beaulieu and Gainetdinov, 2011).

Based on the opposite action exerted on this signalling cascade, DARs are classified in two main classes. D1-like class receptors are coupled to the G protein subunit $G\alpha_{s/olf}$ and include the receptor types D1 and D5. When DA binds to D1/5R, $G\alpha_{s/olf}$ activates AC, which in turn stimulates the production of the second messenger cAMP and the phosphorylation of protein kinase A (PKA, pPKA). On the opposite side, cAMP and pPKA levels are reduced when DA interacts with the D2-like class receptors. This class includes the receptor types D2, D3 and D4, which signalling cascade is mediated by the inhibitory subunit $G\alpha_i$ (Sibley et al., 1992).

Among all five DARs, D1Rs and D2Rs are the most abundant in the striatum. Despite several studies confirming the colocalization of D1Rs and D2Rs in a small subpopulation of SPNs (Lester et al., 1993; Meador-Woodruff et al., 1991; Surmeier et al., 1992; Surmeier et al., 1996), the two receptors are generally found segregated in the dSPNs and iSPNs respectively (Valjent et al., 2009). Thus, DA binding to D1Rs and D2Rs will not only result into opposite modulation of direct and indirect pathway neurons activity, but also into different output signals arising from the BG network. Briefly, DA activates dSPNs and inhibits iSPNs by its binding to D1R and D2R in that order. Network-wise, the result of DA action on D1R and D2R-containing neurons is the inhibition of the BG output structures and the disinhibition of the thalamic nuclei.

It is also important to mention that, while D1Rs in the striatum are exclusively expressed in the dSPN, D2Rs are not exclusive of one population cell type. In fact, D2Rs are also found in the membrane of cholinergic interneurons (Maurice et al., 2004) and in the pre-synaptic membrane of both corticostriatal glutamatergic terminals (Bamford et al., 2004) and in the terminals of midbrain DA neurons (Ford, 2014). When distributed pre-synaptically, D2Rs work as autoreceptors, providing an important negative feed-back mechanism that adjust the neurotransmitter release in response to changes in the extracellular DA levels (Sibley and Monsma, 1992).

The remaining subtypes, D3R, D4R and D5R, are also present in the striatum but less abundantly expressed in comparison to the first two receptors of the

family. D3Rs are mainly express in direct pathway SPNs of the ventral striatum (Ridray et al., 1998), where they exert a synergistic effect on D1Rs through direct intermembrane interaction (Marcellino et al., 2008). Immunolabelling of D4Rs in the rat striatum revealed an heterogenous expression of the receptor protein, which is preferentially enriched in the striosomal compartment (Rivera et al., 2002b). Last, D5Rs are rare to find in GABA-ergic neurons while their expression is mainly restricted to large striatal neurons, such as cholinergic, parvalbumin and somatostatin positive interneurons (Rivera et al., 2002a).

Dysfunctions of the basal ganglia

Dysfunctions or lesions in the BG result either in an overall decreased motor output (akinesia/hypokinesia and bradykinesia) or in excessive uncontrollable movements (dyskinesia). Both movement disorders occur in Parkinson´s disease (PD), where akinesia is one of the cardinal disease symptoms whereas dyskinesia is a complication of L-DOPA pharmacotherapy. Current pathophysiological models attribute akinesia and dyskinesia to opposite imbalances in the activity of a movement-promoting and a movement-suppressing pathway linking the striatum with deeper basal ganglia nuclei (see Figure 3).

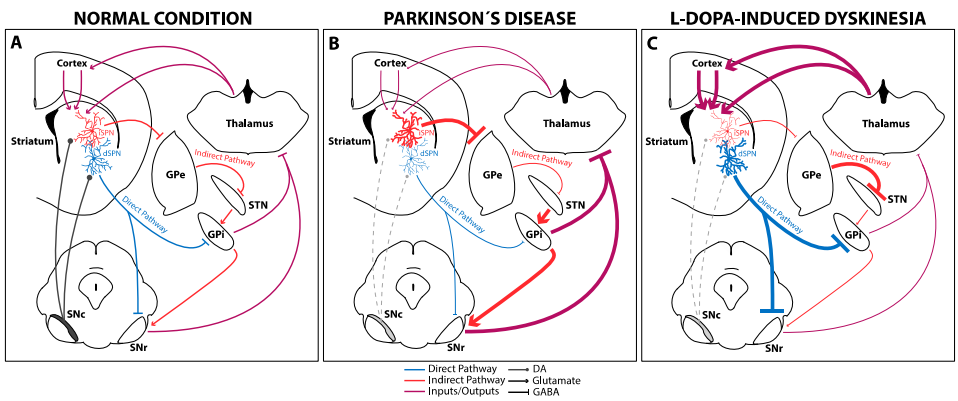

Figure 3: Graphic representation of the BG circuit in health, DP and LID: Exitatory glutamatergic inputs from the cortex and the thalamus (purple arrows) together with DA-ergic inputs from the SNc (grey arrows) converge to the SPN of the striatum. In the striatum, GABA-ergic projections of the SPNs give rise to the the direct (dSPN) and the indirect (iSPN) pathway. dSPNs project directly to the output nuclei GPi and SNr (blue arrows) wheras iSPN, reach to the same output nuclei indirectly via the intermediate nuclei GPe and STN (red arrows). GPi and SNr project to the thalam and the cortex completing the loop. In health brain DA maintains balance in the circuit (A). In PD, the neurodegenerive process that affects the DA-producing neurons in the SNc causes a reduction of DA content in the striatum (dashed grey arrows). This results in relative hyperactivity of the inderect pathway and reduced activity of the direct pathway (B). LID on the contrary is mainly associated to the hyperactivity of the direct pathway (C).

Parkinson´s disease

It was more than two hundred years ago when within a 66 pages essay, James Parkinson presented a vivid description of six aged man who suffered from a progressive disease characterized by unusual motor complications (Parkinson, 2002). The disease he firstly described to the scientific community as the syndrome of the "shaking palsy", today bears its name and is the second most common neurodegenerative disorder worldwide.

PD is an ensemble of motor and non-motor features that are causally linked to the progressive loss of dopaminergic neurons in the SNc and the resultant drop of DA content in the brain. The motor symptoms originally described by James Parkinson (bradykinesia, rigidity, tremors at rest and postural instability), are still the hallmark of PD (Fahn, 2003) but they only appear at the advanced stage of the disease, when the degenerative process has already affected 30% of nigral neurons and 50-70% of striatal DA terminals (Brooks, 2006; Carlsson et al., 1957; Fearnley and Lees, 1991; Greffard et al., 2006; Kordower et al., 2013; Meder et al., 2019). Non-motor symptoms on the contrary, do not require that level of neurodegeneration and often precede the development of motor features; having potential utility for early diagnosis (even though they lack PD specificity per se). It should be notated that non-motor features of PD have a complex pathogenesis, involving neurotransmitter systems other than DA to a large degree.

Nearly 200 years of research and yet, the etiology of PD remains unclear. As 90% of PD cases are idiopathic (while the remaining 10% have genetic connections), it is a widely accepted concept that DA-ergic neurons in the SNc are vulnerable to a range of genetic, molecular, and environmental factors that independently or cooperatively can cause cell death over time (Sulzer, 2007).

Dopamine replacement therapy

Despite no available treatments can stop the neurodegenerative process in PD, DA replacement therapy with the monoamine precursor L-DOPA remains the most effective strategy for alleviating the motor symptoms associated with the disease (Cenci et al., 2011; Cotzias et al., 1969).

Unfortunately, L-DOPA is also a very difficult molecule to control therapeutically particularly because it has a very short half-life. After an initial period of full efficacy, long term treatment with the "miracle drug" is often complicated by the appearance of abnormal involuntary movements, dyskinesias, together with motor fluctuations, "on-off" effects after each L-DOPA dose where patients experience a short-lived benefit followed by a dramatic and sudden return to a parkinsonian state (Cenci et al., 2020; Thanvi et al., 2007). The short half-life of L-DOPA and the motor complications associated with this therapy have led many physicians to favour the use of more stable DA agonists. DA agonists are

often prescribed as an initial treatment, to patients in the early phase of PD, or given in combination with L-DOPA, in more advanced PD stages.

DA agonists are commonly classified into two different categories: (I) ergot derivative, such as bromicriptine, known for their broader spectrum of receptors interaction (D1- and D2-like class receptors, serotonergic and adrenergic receptors); (II) non-ergot derivatives, such as apomorphine, pramipexole, ropinirole and rotigotine, with higher affinity for the D2-like receptors (D2R, D3R and D4R) (Cerri and Blandini, 2020).

Although less dyskinesiogenic than L-DOPA, treatments with selective DA receptor agonists are also less effective in relieving PD motor symptoms and they have been associated with a large palette of unpleasant side effects. For example, it has been estimated that around 14-17% of PD patients on non-ergot DA agonist treatment (D2/3R action) develop impulse control disorders such as gambling, compulsive shopping, sexual behaviour, and abnormal eating disorder (Vargas et al., 2019; Voon et al., 2017). Likewise, the clinical applicability of ergot derivatives has been limited by their scarce brain penetration properties and the large range of receptor interactions (Cerri and Blandini, 2020).

Other administration routes and drug combination strategies are often used to extend L-DOPA half-life and to reduce the variations in drug levels that are associated with motor complications. One example is the inhibitor of the aromatic amino-acid decarboxylase, carbidopa, which is commonly administered together with L-DOPA and prolongs the drug half-life of about 30 minutes. Other drugs, such as inhibitors of the enzymes catechol-O-methyltranferase or monoamine oxidase, can extend L-DOPA availability even further, although they have not yet been proven capable of preventing the development of motor complications (Cenci et al., 2020).

Dyskinesia and dystonia in PD

Abnormal involuntary movements (AIMs) that arise as the complications of L-DOPA pharmacotherapy in PD are better known with the name of L-DOPA-induced dyskinesia (LID). The overall prevalence of LID is high, reaching up to 80% of the total number of PD patients treated with L-DOPA (Cenci et al., 2020; Manson et al., 2012; Muller and Russ, 2006; Thanvi et al., 2007). The risk to develop these motor complications is strictly correlated to both age of onset, disease severity, duration and dose of L-DOPA treatment (Thanvi et al., 2007).

The most typical clinical features of LID are chorea (hyperkinetic dance-like movements) and dystonia, slow movements and abnormal postures caused by sustained muscle contractions (Fahn, 2000). Chorea/choreoathetosis affecting face, neck, arms, trunk and legs are the most common form of LID. They are typical manifestations of “peak-dose dyskinesias” as their appearance occurs when L-DOPA concentration in the bloodstream is high (30-200 minutes after intake of an oral dose). Although dystonia may also be present during peak dose dyskinesia,

the slow twisting postures are often shadowed by the presence of much wider and rapid choreatic movements (Fahn, 2000). The so-called diphasic dyskinesias, which manifest during the rising and falling of L-DOPA plasma levels after each dose, generally have a predominantly dystonic character. Pure isolated dystonia can appear distant in time from the last L-DOPA administration when L-DOPA concentration is low in the system (so called "off-state"). Off-state dystonias are generally painful and affect the lower extremities of the body, the most typical form being early morning foot dystonia (Bezard et al., 2001; Melamed, 1979; Thanvi et al., 2007).

While LID results from L-DOPA pharmacotherapy, dystonia in PD can also become manifest in the absence of dyskinesia, years before the starting of L-DOPA therapy (Albanese et al., 2013; Fahn, 1988). Early dystonia affects 30% of the parkinsonian patients, being even more prevalent in young onset PD (i.e., patients with age below 40 at diagnosis) (Ishikawa and Miyatake, 1995; LeWitt et al., 1986). Early dystonia in PD generally involves the lower limb segments and can manifest while walking, as sustained limb exension and/or fixed contractures (Shetty et al., 2019).

Importantly, the response of early dystonia to treatment with L-DOPA or DA agonists is variable between patients, as it can improve, worsen, or remain unchanged (LeWitt et al., 1986). Similar to the pharmacological approach, deep-brain-stimulation (DBS) has also generated contradictory results in the treatment of dystonia. For instance, chronic GPi-DBS has proven to be beneficial in a small cohort of patients with generalized dystonia (Cersosimo et al., 2009), but also paradoxically lead to parkinsonisms when treating focal dystonia (Zauber et al., 2009).

Striatal signalling in L-DOPA-induced dyskinesia

After more than 50 years of research on L-DOPA use (Cotzias et al., 1969), there is now the consensus that the development of LID is triggered by intermittent and large fluctuations of brain DA levels as engendered by the standard oral treatment with L-DOPA. These waves of DA lead to the abnormal stimulation of the receptors expressed both pre- and post-synaptically in the striatum, with aberrant activation of downstream signalling cascades (Cenci, 2014; Kordower et al., 2013; Olanow et al., 2020). It should however be pointed out that L-DOPA does not cause these large swings in brain DA levels if the nigrostriatal DA system is intact. Indeed, DA neurons are able to maintain the extracellular concentration of DA within a physiological range thanks to multiple regulatory mechanisms. L-DOPA-dependent fluctuations in brain DA levels emerge upon substantial loss of nigrostriatal DA neurons. Under these conditions, L-DOPA gets converted to DA by other cells in the brain (particularly by serotonin neurons, which release this newly formed DA in an unregulated fashion (Cenci, 2014).

Alterations of the striatal D1R signalling pathway

Supersensitivity of the dSPN-D1R towards DA has long been hypothesized as a crucial determinant to the development of LID (Gerfen, 2003). In both animal models and PD patients, the long absence of physiological DA levels in the striatum stimulates the production of $G\alpha_{s/olf}$ protein (Alcacer et al., 2012; Herve et al., 1993) contributing to the upregulation of signalling cascades downstream the D1R (Aubert et al., 2005; Sebastianutto et al., 2020; St-Hilaire et al., 2005). Furthermore, $G\alpha_{s/olf}$ levels are maintained high during LID, and positively correlate with the severity of dyskinesia (Alcacer et al., 2012; Corvol et al., 2001). However, partial genetic ablation of the stimulatory α subunit in transgenic mice has failed to reduce dyskinesia, suggesting that $G\alpha_{s/olf}$ upregulation and LID have no causal relationship but instead results from the activation of downstream signalling pathways (Alcacer et al., 2012). As a matter of fact, in both animal models and PD patients the aberrant activation of D1Rs during LID results in a remarkable increase in the levels of cAMP and PKA-dependent phosphorylation of downstream targets, including the GluA1 subunit of the amino-3-hydroxy-5-methyl-4-isoxazolepropionic acid receptor (AMPAR) (phosphorylated at the Ser^{845} residue) (Snyder et al., 2000), the dopamine- and cAMP-regulated neuronal phosphoprotein (DARPP32) (phosphorylated at the Thr^{34} residue) (Santini et al., 2007) and the extracellular signal-regulated protein kinase 1 and 2 (ERK) (phosphorylated at the $Thr^{202/204}$ residues) (Santini et al., 2009; Westin et al., 2007).

In normal physiological conditions the conversion of ERK into its active phosphorylated form (pERK) is associated to the stimulation of kinases or glutamate receptors and not to $G\alpha_{s/olf}$ (Gerfen et al., 2002), and serves the role of an important regulator of gene transcription and protein translation. On the contrary, in dyskinetic animals, aberrant ERK activation in the lesioned striatum takes place selectively in dSPNs and is also modulated by the $G\alpha_{s/olf}$ pathway (Pavon et al., 2006; Westin et al., 2007). When pERK signalling increases in the dSPNs, it triggers chromatin remodelling mediated by the active phosphorylated form of histone 3 (H3) (Santini et al., 2009) and profound maladaptive changes in the transcriptional regulation. Dependent on ERK activity is also the production of transcription factors like c-Fos, FosB/ΔFosB, JunB and c-Jun. All these transcription factors are induced by the rapid activity of immediate early genes (IEG) and accumulate in the DA-denervated dSPNs of dyskinetic rodents chronically treated with L-DOPA (Cenci et al., 1999; Pavon et al., 2006; Westin et al., 2001).

Pharmacological and genetic inactivation of striatal D1Rs and its downstream targets have succeeded in ameliorating dyskinesia in experimental animal models of LID (Bateup et al., 2010; Darmopil et al., 2009; Lebel et al., 2010; Oh et al., 1997; Santini et al., 2012; Santini et al., 2007). At the same line, a selective dSPNs activation via optogenetic stimulation could induce dyskinesias in rodent models of PD even in the absence of L-DOPA (Girasole et al., 2018; Keifman et al., 2019;

Ryan et al., 2018). During several years, all these results have contributed the idea that dSPNs overactivity is necessary and sufficient for the development of LID.

Role of striatal D2R in PD and LID

While most of the studies on LID were focusing on the role of D1Rs, the role of D2Rs in dyskinesia remained underrated for decades. Conversely, well-known are the drastic readaptations that striatal D2Rs undergo after DA depletion and how these changes strongly drive the parkinsonian motor symptoms. In 1990, Gerfen and collaborators showed that following striatal DA loss, there is an increase in the D2R mRNA expression and in the production of enkephalin, a neuropeptide selectively expressed in the iSPNs (Gerfen et al., 1990). Later on, studies performed on experimental models of PD, linked the loss of DA signalling to phenomena of homeostatic readaptations that eventually effect the iSPN intrinsic excitability and dendritic spine density; which were both found restored only in dyskinetic animals after treatment with L-DOPA (Fieblinger et al., 2014a; Zhang et al., 2013). Finally, the link between striatal D2Rs and the development of PD-like behaviour was demonstrated with studies addressing the impact of a genetic D2Rs ablation on the motor performances of DA-intact mice. Mice affected with either a global or more specific iSPN-targeted knock-out (KO) for the D2R were reported to experience severe parkinsonism such as reduced locomotion and longer periods of immobility (akinesia and bradykinesia) (Bello et al., 2017; Kelly et al., 2008; Lemos et al., 2016).

What about D2Rs and dyskinesia? What do we know so far? There is a lot of confusion and contrasting data around D2Rs in dyskinesia and one reason is probably that D2R agonists still play an important role in the treatment of human PD (addressed in the previous chapter). Moreover, studies performed on animal models of LID have reported contrasting results, between different species and even when using the same experimental model. For example, a few studies have showed that D2/D3R agonists can induce conspicuous AIMs in parkinsonian rats (Bagetta et al., 2012; Shin et al., 2014), whereas others have reported only mild or no dyskinesia unless rats were previously primed with L-DOPA (Carta et al., 2008; Lundblad et al., 2002). Priming is defined as the process by which the first stimulation of a DA receptor in the DA denervated brain modifies the response to subsequent dopaminergic treatments (Morelli et al., 1989). Furthermore, parkinsonian mice genetically deprived of D2Rs and treated with L-DOPA were reported to develop levels of dyskinesia that were not different in severity from those observed in wild type (WT) animals (Darmopil et al., 2009). Differently from the rodent model, numerous studies in macaque monkeys do not support the view of D1R activation as the sole mechanisms mediating LID, but rather suggest that both D1R and D2R stimulation might be equally important in this species (Gomez-Mancilla and Bedard, 1992; Luquin et al., 1994). Interestingly, one of the

above mentioned study reported that D2R stimulation in macaque monkeys can only cause dystonia and not chorea (Boyce et al., 1990a).

Alterations of glutamate system in LID

Glutamate is the most abundant excitatory neurotransmitter in the brain and both DA depletion and DA replacement therapy can profoundly alter its transmission within the BG network (Calabresi et al., 2007; Chase and Oh, 2000; Sebastianutto and Cenci, 2018; Sgambato-Faure and Cenci, 2012). This is not surprising considering that the membrane of striatal SPNs accommodates all types of glutamate receptors. In physiological conditions, the cross talk between DA and glutamate signalling is essential to regulate patterns of neuronal firing, protein phosphorylation and gene expression. In experimental PD, the loss of DA results in enhancement (long term potentiation) and depression (long term depression) of glutamatergic transmission in indirect and direct SPNs respectively; thus reflecting decreased levels of glutamate release (Shen et al., 2008). Conversely in LID, an increased concentration of extracellular glutamate has been observed in both striatum and SNr, suggesting a general overactivity within the BG circuitry (Boulet et al., 2006; Robelet et al., 2004).

Ionotropic receptors, fast ligand-gated ion channels, such as the N-methyl-d-aspartate receptor (NMDAR), AMPAR and the kainite receptor, mediate fast glutamate excitatory neurotransmissions within the BG. Amantadine is a multi-target drug with antagonistic activity at the NMDAR used in both early and advanced stages of PD. This drug is well-known for its prokinetic and anti-dyskinetic properties (Metman et al., 1999), but also associated to severe aversive effects such as hallucinations, delusion and depression (Cummings, 1991; Fox et al., 2011).

Like DA, glutamate can also activate GPCRs. Based on structural similarities and on the α subunit that binds to the intracellular domain, metabotropic glutamate receptors (mGluR) are distinguished in three groups: group I, II and III (Sebastianutto and Cenci, 2018). Group I receptors, mGluR1 and mGluR5, are found in the post-synaptic membrane of striatal neurons where they couple to the activating G_q protein. The interaction of glutamate to these receptors activates phospholipase C (PLC) and protein kinase C (PKC) leading to an increase of intracellular calcium (Ca^{2+}) levels (Pin and Acher, 2002). The mGluR5 type is highly expressed in both interneurons and SPNs, but only in the latter population the receptors number exponentially increases during dyskinesia (Konradi et al., 2004; Ouattara et al., 2011). For this reason, drugs that potentially inactivate mGluR5 activity have emerged as promising treatment for dyskinesia. One example is the selective mGluR5 antagonist MTEP (3-(2-methyl-4-thiazolyl) ethynyl pyridine) which in animal models of LID has been reported to improve peak dose dyskinesia and decrease the abnormal ERK activation in the dSPNs (Fieblinger et al., 2014b; Iderberg et al., 2013; Morin et al., 2013; Rylander et al.,

2010). In line with the pre-clinical studies, clinical trials using negative allosteric modulators (NAMs) of the mGluR5, have also proven to be beneficial in PD patients with moderate to severe dyskinesia. Regardless of the promising results, long treatment periods with NAMs also relates to several adverse effects such as dizziness, hallucinations and insomnia, or even to the worsening of dyskinesia when the treatment is interrupted (Sebastianutto and Cenci, 2018).

Group II and III mGluRs inhibit cAMP and PKA signaling as they are coupled to the $G_{i/o}$ protein. Group II receptors, mGlu2R and mGlu3R, are mainly expressed at the cortico-striatal and subthalamo-nigral terminals, while Group III receptors, mGluR4, mGluR6, mGluR7 and mGluR8, are found in the terminals of striatal GABA-ergic neurons (Bradley et al., 1999).

Aims of this thesis

Aims of this thesis

I. To address the role of dSPNs and iSPNs in different motor behaviours using cell-type specific chemogenetic stimulation (Paper I).

II. To elucidate the signalling mechanisms that mediate D1R-dependent aberrant ERK activation in the DA-depleted striatum (Paper I and Paper II) and to investigate the functional interaction between D1R and mGluR5 as a possible target for the treatment and prevention of LID (Paper II).

III. To develop a new rating scale for assessing dystonic features in the mouse models of LID and to examine the patterns of dyskinetic and dystonic features induced by pharmacological D1R versus D2R stimulation (Paper III).

IV. To examine the specific contribution of iSPN-D2R in generating parkinsonian and dyskinetic features using targeted receptor gene manipulations (Paper IV).

Materials and Methods

Materials and Methods

Animals

Rodent models of PD and LID were used in the present thesis. Both WT and genetically engineered transgenic mice were used within the four studies. Specifically, two lines of bacterial artificial chromosome (BAC) transgenic mice were used in Paper I to selectively target the two SPN populations in the striatum: BAC-*Drd1a*-Cre (D1-Cre, GENSAT project, founder line EY262) and *Adora2a*-Cre mice (A2a-Cre, GENSAT project, founder line KG139), for D1R and D2R-SPN expressing neurons, respectively. Paper II includes both WT mice and two transgenic mouse lines where mGluR5 expression was knocked-down (KD) (KD mice, mGluR5$^{KD\text{-}D1}$) or completely abolished (KO mice, mGluR5$^{KO\text{-}D1}$) in the D1R-exressing SPNs. The generation process of the mGluR5$^{KD\text{-}D1}$ line is extensively described in (Novak et al., 2010) while KO mice were generated by crossbreeding homozygous mGluR5$^{loxP/loxP}$ mice (Xu et al., 2009) with heterozygous D1-Cre mice. Male and female WT mice purchased from Charles River were used in Paper III. Paper IV involved the dSPN-reporter mouse line BAC-*Drd1a*-tdTomato (GENSAT) (Shuen et al., 2008), *Drd2*$^{loxP/loxP}$ homozygous mice (B6.129S4 FVB-Drd2tm1.1Mrub/J, JAX020631, JAX) and A2a-Cre mice.

Furthermore, *Drd2*$^{loxP/loxP}$ homozygous mice and A2a-Cre mice were crossbred to generate mice with different levels of iSPN-D2R depletion, as previously described in (Dobbs et al., 2016) and (Lemos et al., 2016). Female rats of the Sprague Dawley strain used in Paper II were purchased from Charles River and weighted approximately 200-225 g at the beginning of the experimental procedures. All mice were kept on C57B6 background and were randomized for both genders. Mice were approximately 10-12 weeks of age at the beginning of the experimental procedures. All animals were housed under 12 hours light/dark cycle with *ad libitum* access to food and water.

Table 1: overview of the transgenic mouse lines used in the four studies.

Mouse Colony	Promoter	Transgene	Description	Paper
Adora2a-Cre	Adora2a	Cre	iSPN reporter	I, II
Drd1a-Cre	Drd1a	Cre	dSPN reporter	I
BAC-Drd1a-tdTomato	Drd1a	tdTomato	dSPN reporter	I, IV
mGluR5^{KD-D1}	Drd1a	mGluR5 - iRNA	mGluR5 knock-down in dSPNs	II
mGluR5$^{loxP/loxP}$	Grm5	mGluR5^{loxP}	mGluR5 gene is flanked by loxP sites	II
Drd2 $^{loxP/loxP}$	Drd2	Drd2 ^{loxP}	D2R gene is flanked by loxP sites	IV
C57B6	-	-	WT mouse	II, III, IV

Surgical procedures

Animal model of PD

Chronic striatal DA denervation was induced through the injection of the neurotoxin 6-hydroxidopamine (6-OHDA, Sigma Aldrich) in the right medial forebrain bundle (MFB) both in mice and rats according to the well-established methods (Cenci and Lundblad, 2007; Francardo et al., 2011). Briefly, the toxin was dissolved at a fixed concentration of 3.2 µg/µL (calculated from free base weight) in 0.02% ice-cold ascorbic acid saline solution and used within two hours. In mice (Paper I-IV) of 1 µL toxin solution was injected at the following coordinates (in mm relative to bregma and dural surface): antero-posterior (AP) = -0.7, medio-lateral (ML) = +1.2, dorso-ventral (DV) = -4.7. Tooth bar was adjusted accordingly to reach flat-skull position. In rats (Paper II), two injections of 2.5 and 2 µL volume respectively were performed at the following coordinates (in mm relative to bregma and dural surface): (1) AP = -4.4, ML = -1.2, DV = -7.8; (2) AP = -4.0, ML = -0.8, DV = -8.0. The incisor bar was lowered to -4 position or adjusted individually for flat-skull position. Rats and mice with a complete DA denervation of the striatal motor regions exhibited ≤ 30% contralateral forelimb use in the cylinder test and were therefore included in the studies (Francardo et al., 2011; Lundblad et al., 2004). Furthermore, the success of the striatal denervation was verified post-mortem using TH immunohistochemistry. Rats and mice included in the studies had ≥ 85-90% reduction in the density of striatal DA fibers terminals in the lesioned side compared to the non-injected hemisphere.

Chemogenetic manipulation

The chemogenetic technology of designer receptors activated by designer drugs (DREADDs) is a powerful and non-invasive method to control intracellular signalling pathways and activity of targeted cell populations both in-vivo and in vitro (Rogan and Roth, 2011). DREADDs are genetically modified muscarinic receptors which are evolved to no longer respond to acetylcholine or any other endogenous ligands, but exclusively to the inert and inactive clozapine metabolite clozapine N-oxide (CNO) (Armbruster et al., 2007).

There are four main types of DREADDs and each one allows for chemogenetic activation of different canonical (G-protein-mediated) and non-canonical (β-arrestin-mediated) signalling pathways: the activatory hM3Dq (Gq-DREADD), rM3Ds (Gs-DREADD) and rM3DArr (β-arrestin-preferring-DREADD) receptors, and the inhibitory hMD4i (Gi-DREADD) receptor.

The G_q type hM3Dq was the first DREADD to be designed and originated from two-point mutations of the human muscarinic M3 receptor (Rogan and Roth, 2011). Later, other two G_q-DREADDs were developed from different human muscarinic receptors, hM1Dq and hM5Dq. hM3Dq is however the most widely used (Roth, 2016). G_q-DREADDs signal through the $G_{\alpha q/11}$ protein, and therefore increase intracellular Ca^{2+} levels in a PLC-dependent manner (Alexander et al., 2009).

On the contrary, G_i-DREADD signaling cascade is mediated via the $G_{\alpha i/o}$ protein, which mediates neuronal silencing through downregulation of AC activity and decrease in cAMP production (Armbruster et al., 2007). Currently, there are three G_i-DREADDs available: two are based on human muscarinic receptors and are activated by CNO, hM2Di and hM4Di (the most widely used); the other one derives from the human κ-opiod receptor, KORD (Roth, 2016) and is activated by another inherent drug: salvinorin B (Vardy et al., 2015).

The activatory G_s-DREADD signals through the $G_{\alpha s}$ protein (Farrell et al., 2013) and is a chimera of the rat muscarinic M3 receptor and the intracellular region of a turkey erythrocyte β-adrenergic receptor (Dong et al., 2010).

Last, the DREADD receptor that couples to β-arrestin derives from the human M3 muscarinic receptor and activates non-canonical signaling cascades that are independent from G-proteins activity (Nakajima and Wess, 2012). Because its activation requires high CNO concentrations in-vivo, the range of applications offered by this receptor are limited (Roth, 2016).

In Paper I, we used a double-floxed inverted open reading frame strategy (DOI) to express the activatory G_q- or G_s-DREADD selectively in SPNs of the mouse striatum. Specifically, DREADDs were delivered via unilateral injection of Cre-recombinase (Cre) -inducible viruses into the DA intact or the DA-depleted striatum of Cre-transgenic mice. D1-Cre and A2a-Cre mice were used to target dSPNs and iSPNs respectively. DREADD and control plasmids were purchased

from the university of North Carolina at Chapel Hill and packaged at the Lund university AAV Vector Core into three different serotype 5 adeno associated viral vectors (AAV): AAV5-hSyn-DIO-hM3DqmCherry (G_q-DREADD), AAV5-hSyn-DIO-rM3Ds-mCherry (G_s-DREADD), and AAV-hSyn-DIOEGFP-WPRE (control vector). Vector titers were in the range of 9.9 x 10^{13} to 4 x 10^{14} at working concentration. Vector preparations were diluted ten times and delivered into the right dorsolateral striatum with two injections (1 µL each) performed at the following coordinates (flat-skull position): (1) AP = +1.0, ML = -2.1, DV = -2.9; (2) AP = +0.3, ML = -2.3, DV = -3.0.

Viral-mediated receptor KO strategy

In Paper IV, we used a virally-mediated Cre/loxP strategy to generate a new mouse model with conditional KO for the iSPN-D2Rs (D2RKO). Briefly, to induce a selective KO for the D2R gene (*Drd2*) in the iSPNs, transgenic homozygote *Drd2*$^{loxP/loxP}$ mice were transfected into the right striatum with a viral construct driving the expression of Cre under the control of the preproenkephalin-A (PPA) promoter activity. WT littermate derived from the *Drd2*$^{loxP/loxP}$ colony underwent the same surgical intervention and were used as control group. After receiving the AAV injection, *Drd2*$^{loxP/loxP}$ and WT mice were named respectively AAV-Drd2KO and AAV-Drd2WT mice. The Cre-expressing AAV vector was packaged into a serotype 5 (AAV5-PPA-Cre) and diluted thirty times in a vector preparation that was delivered into the right striatum with two injections (1 µL each) at the following coordinates (flat-skull position): (1) AP = +1, ML = -2.1, DV = -2.6; (2) AP = +0.3, ML = -2.3, DV = -2.6. Moreover, a Cre-inducible AAV5-flex-GFP viral vector was injected in combination (diluted 10 times) with the AAV5-PPA-Cre construct in BAC-*Drd1a*-tdTomato mice to label Cre positive cells in green. Titration of the two vectors was in the range of 1.8 x 10^{14} and 3.3 x 10^{14} for AAV5-flex-GFP and AAV5-PPA-Cre respectively. Plasmids and vectors were produced at the Lund university AAV Vector Core.

Drugs

An overview of the compounds (and respective vehicle controls) administered in-vivo is reported in table 2. For detailed protocols regarding solutions preparation and drugs solubility please refer to the method section of the Papers I-IV.

Table 2: list of the compounds administered in-vivo.

Drug	Receptor target	Principle of action	Dose	Animal model	Supplier	Vehicle	Inj. route	Paper
L-DOPA	DAR	Agonist	1/3/12 3/6 6	Mouse Mouse Rat	Sigma Aldrich	Saline + benseraz.	i.p. i.p. s.c	I II/III/IV II
SKF38393	D1/5R	Partial agonist	3/6 2 3	Mmouse Rat Mouse	Sigma Aldrich	Saline	i.p. s.c i.p.	II/III II IV
Quinpirole	D2/D3R	Agonist	0.5 0.5/1	Mouse Mouse	Tocris	Saline	i.p i.p	I/IV III
Sumanirole	D2R	Agonist	2/4 4	Mouse Mouse	Tocris	Saline	i.p i.p	III IV
SCH23390	D1/5R	Antagonist	0.05	Mouse	Tocris	Saline	i.p	III
L741626	D2R	Antagonist	4	Mouse	Tocris	Saline+ NaOH+ Acetic acid	i.p.	III
MTEP	mGluR5	Antagonist	5	Mouse/rat	Abcam	Saline+ 5%DMSO	s.c	II
U73122	PLC	Inhibitor	10 30	Mouse Rat	Tocris	Saline+ 5%DMSO	s.c. s.c	II II
U73343	Inhactive form of U73122	-	10 30	Mouse Rat	Tocris	Saline + 5%DMSO	s.c s.c	II II
Dicyclomide hydrocloride	Muscarinic receptor	Antagonist	15	Rat	Sigma Aldrich	Saline	i.p.	II
CNO	DREADD	Agonist	1/2/5	Mouse	Tocris	Saline + 5%DMSO	i.p.	I

Behavioural testing

Abnormal involuntary movements (AIMs) ratings

In unilateral mouse and rat models of PD, dyskinesias are recognized as movements that are (I) induced by L-DOPA or other DA agonist treatments, (II) occurring on the side of the body contralateral to the lesion, (III) repetitive, purposeless, and not recognizable within the normal rodent behavioural pattern (Cenci et al., 1998). Two well-established scales were used to discriminate and rate dyskinesia severity in mice (Francardo et al., 2011) and rats (Cenci et al., 1998; Lundblad et al., 2004) in Papers I, III and IV and in Paper II, respectively.

Both scales consider three subtypes of AIMs based on their topographic distribution: axial AIMs are twisting-bending movements affecting the neck and the upper body region, limb AIMs are jerky and fluttering movements of the forelimb, while orofacial/orolingual AIMs are defined as rapid contractions of jaw and facial muscles with or without tongue protrusion. Mice and rats were placed in

individual transparent cages starting from 10-20 minutes before drug administration (habituation period) to avoid unwanted stress related to the new environment. After receiving the injection treatment, AIMs were observed for 1 minute every 20 minutes for a total duration of 180 minutes. Dyskinesia in mice was rated on a severity scale from 0 to 4, based on the duration (frequency scale) of each AIM subtype within the 1 minute observation period (0 = no dyskinesia; 1 = occasional signs of dyskinesia present for less than 50% of the observation time; 2 = frequent signs of dyskinesia present for more than 50% of the observation time; 3 = dyskinesia present during the entire observation period but easily interruptible by external stimuli; 4 = continuous dyskinesia not interrupted by external stimuli). In the rat, the frequency scale was combined with an amplitude scale (also with grades from 0 to 4) describing the degree of deviation of the dyskinetic body parts from their resting position. The combination of frequency and amplitude scores is indicated with the term global AIM scores (severity scores multiplied for amplitude scores for each observation point).

Dystonia ratings

In Paper III, we introduce a new rating scale for the detection of dystonic abnormal movements and postures in the mouse. Dystonic features that fulfilled the phenomenological definition of dystonia (sustained or intermittent muscle contractions causing abnormal movements, postures, or both (Albanese et al., 2013)) were considered by the scale only when sustained for a period ≥ 2 seconds. Half point scores ranging from grade 0 to 3 were assigned to different body segment using a scale that anchored the frequency of movements/postures to actual number of seconds (0 = no signs of dystonia; 0.5 = single or occasional dystonic events occurring for less than 10 seconds; 1 = signs of dystonia present for 11 to 20 seconds; 1.5 = signs of dystonia present for 21 to 30 seconds; 2 = signs of dystonia present for 31 to 40 seconds; 2.5 = signs of dystonia present for 41 to 50 seconds; 3 = signs of dystonia present for 51 to 60 seconds).

Dystonia ratings were performed offline from the observation of videos recorded during each dyskinesia session (action camera: GoPro Hero 4, GoPro Inc., USA). Based on their topographical distribution dystonic features were classified in four main subtypes: trunk/neck (Tr/ne) dystonia, forelimb (contralateral or ipsilateral to the lesion, cFL and iFL) dystonia, hindlimb (contralateral or ipsilateral to the lesion, cHL and iHL) dystonia, and Straub tail (Tail) dystonia. For a detailed description of the dystonic traits related to each body part and included in the rating, please refer to Paper III, results section, Table 2.

Cylinder test

A test of spontaneous limb use during vertical exploratory behaviour was used in all experimental mice and rats included in the four studies to assess the level of DA-denervation in the striatum induced by the 6-OHDA lesion (Francardo et al., 2011; Lundblad et al., 2002). This test takes advantage of the animal innate drive to explore a new environment by standing on the hindlimbs and leaning towards the enclosing walls. Briefly, mice and rats were placed individually inside a glass cylinder and video recorder for 5 minutes. Video recordings were analyzed offline to count the number of wall contacts performed with the right or the left forepaw to support the mouse body against the cylinder wall. The performance of the paw contralateral to the lesion (left paw) was expressed as a percentage of the total number of wall contacts taken within 5 minutes session. Moreover, in Paper IV, cylinder test performance of mice from the AAV-Drd2KO and AAV-Drd2WT group were used to assess the effect of the unilateral D2R depletion on the contralateral forelimb usage.

Open field test

In Paper I and Paper IV, mouse motor behaviour was evaluated using a video tracking system (Stoelting ANY-MAZE video tracking) providing measurements of both horizontal and vertical activity. The test, commonly known with the name of open field test, consists of a transparent Plexiglas box (40 cm in diameter) and a camera placed on top of it which detects and records the position of the animal's head, body, and tail at selected time points. All mice were handled and habituated to the injections and to the open field arena for a minimum of two consecutive days (habituation days, 30/60 minutes per training session) prior to the day of the test (2/3 hours per session).

In Paper I, three days of habituation were followed by two consecutive days of testing, where mice were injected with CNO (1 mg/kg) or vehicle according to a randomized crossover design. Mice were first recorded for 60 minutes at baseline (before CNO/vehicle injection) and then recorded for an additional 120 minutes for a total test time of 3 hours. In Paper IV, the test consisted of two days of habituation followed by one single day of test during which animals were recorded at baseline for a total duration of 2 hours. Only in Paper IV, the open field arena was virtually divided in two regions: the center (20x20 cm wide square place in the middle of the arena) and the periphery (leftover area).

Video frames analysis and DeepLabCut

In Paper III, mice were video recorded with a high-speed camera (GS3-U3-23S6C-C, FLIR Grasshopper®3, 140 frames/s) while having normal and drug-

induced abnormal behaviours (dyskinesia and dystonia). An accurate quantification of these behaviours was performed on frozen video frames using the free software FIJI (Schindelin et al., 2012) or via video analysis, using a software for markerless pose estimation (DeepLabCut) (Mathis et al., 2018). Mice were filmed from below while freely moving in a circular arena (33 cm of diameter) placed on top of a transparent glass table. Videos of 2 minutes length were taken every 20 minutes for a total period of 100 minutes after drug or vehicle administration.

Briefly, for the analysis of the frozen frames, 50 frames were randomly extracted from the 2 minutes recording periods and converted into JPEG pictures using an ad-hoc developed algorithm based on Python (Python Software Foundation. Python Language Reference, version 3.9.5. Available at http://www.python.org). Next, we used the "multipoint" tool in FIJI to precisely mark left and right hindpaws. XY coordinates of each marked point were used to calculate the divergence (angle degrees) between the hindlimbs; this measure was defined as "hindpaw angle".

Video analysis with DeepLabCut was used to obtain a geometrical correlate of abnormal trunk/neck posturing, defined as "axial bending", and to monitor the animals´ locomotive pattern inside the circular arena. The DeepLabCut network was trained on 95% of the dataset and tested on 5% of the dataset. The estimated error on the trained and on the tested dataset was < 0.77 and < 1.24 mm, respectively. For each marked point, DeepLabCut provided three columns of data: X coordinates, Y coordinates and detection likelihood. Markers with a likelihood below 0.5 were excluded and replaced with the marker position in the previous frame.

For the analysis of the axial bending an angle was calculated from the intersection between two vectors extending from the mid-point between hindlimbs, to the nose-tip and the tail base, respectively. Next, we examined the patterns of ambulation (distance travelled and speed) in the open-field arena by tracking the animal´s body centroid. For each frame of the 2 minutes recording period, the centroid was defined as the midpoint between 6 body parts: nose tip, left and right forelimbs, left and right hindlimbs, and base of the tail.

Ex-vivo experiments

Protein ligation assay

Coronal striatal sections (50 μm thick) from rats and mice (WT and mGluR5KO-D1), were blocked with 10% horse serum and permeabilized with 0.2% Triton X-100. Signal for protein-protein interaction was then visualized according to the manufacturer's instructions (Duolink & PLA Technology, Olink-Bioscience)

(Fredriksson et al., 2002). Briefly, sections were incubated with D1R primary antibody conjugated to minus Duolink II PLA probes and with mGluR5 primary antibody at 4°C for approximately 36-48 hours. Secondary antibodies PLA probes plus conjugated with oligonucleotides were added and let incubate for 1 hour at 37°C. After DNA amplification, the detection of the signal was carried out using the fluorescent 624 Duolink in situ detection Kit. Fluorescent signal was analysed using a 40x objective (oil immersion) mounted on a confocal microscope.

InsP assay in slices

Inositolmonophosphate (InsP) formation was measured in striatal rat tissue prelabelled with the tritiated precursor [3H]inositol. Briefly, dissected striatal tissue was transferred on ice-cold Krebs-Henseleit buffer at pH 7.4 (118 mM NaCl, 4.7 mM KCl, 1.18 mM MgSO4, 1.18 mM KH2PO4, 24.8 mM NaHCO3, 1.2 mM CaCl2, 10 mM d-glucose) and pre-gassed with 95% O2 and 5% CO2. Slices (350 x 350 µm) were cut using a McIlwain tissue chopper and incubated for 1 hours in a buffer containing 1µCi of myo-[3H]inositol. Next, InsP degradation was blocked with the addition of LiCl (10 mM), while mGluR1 activity was antagonized with the receptor antagonist JNJ16259685 (10 µM). Slices were then treated with either vehicle or ligands (agonists and antagonists) for D1R (SKF38393, agonist) and mGluR5 (DHPG, agonist; MTEP, antagonist) for 60 minutes. Past incubation period, the reactions were stopped by adding methanol/chloroform (2:1) to the solutions. After low speed centrifugation, supernatant containing [3H]InsP was separated by anion exchange chromatography. Finally, samples were allowed to dry at 50°C for 2 hours and protein content measured as described in (Lowry et al., 1951).

Slice preparation and electrophysiological recordings

Acute mouse brain slices were used for electrophysiological recordings in Paper I. Right after extraction, brains were immersed in ice-cold artificial cerebrospinal fluid (aCSF, containing 124 mM NaCl, 3 mM KCl, 26 mM NaHCO3, 120 mM NaH2PO4, 2 mM CaCl2, 1 mM MgCl2, and 16.66 mM glucose) and cut into sagittal slices (275-µm-thick) using a vibrating microtome (VT1200s, Leica, Germany). To maintain a proper pH and oxygenation of the tissue, the aCSF had a molarity of 305 mOsm and was constantly gassed with O2/CO2 (95%/5%). Brain slices were then moved to warm aCSF (33-34 °C) and let recover for about 30 minutes. Slices were then transferred to a submersion-style recording chamber mounted on a Zeiss LSM 710 NLO and kept at room temperature for the whole duration of the experiment. DREADD-transduced SPNs were identified by the presence of EGFP or mCherry fluorescence tag. Whole cell patch clamp recordings were made for 5 minutes at baseline and for 20 minutes after CNO (10

μM) was added to the bath, while cells were stimulated every minute with brief current injections (150 ms).

Tissue preparation and immunohistochemistry/immunofluorescence

After one last injection with the selected drug (for detail refer to Paper I-IV) or vehicle animals were anesthetized with pentobarbital (0,25 ml, 500 mg/kg, i.p., Sanofi-Aventis) and rapidly perfused transcardially with 4% (w/v) paraformaldehyde (PFA) in saline phosphate buffer (PBS), pH 7.4. Brains were post-fixed for 2 hours (rat brains, Paper II) or overnight (mouse brains, Papers I, III and IV) in the same solution and stored at 4°C. Following post-fixation period in PFA, rat brains were moved into a new solution containing sucrose at 25% for 24-36 hours and coronal sections (30 μm thick) were cut on a freezing microtome. Differently, mouse brains were moved directly from PFA to PBS buffer and coronal sections (30 μm thick) were cut using a vibrating microtome (VT1200s, Leica, Germany). All sections were stored at -20°C in a solution containing 30% (v/v) ethylene glycol, 30% (v/v) glycerol, and 0.1 M sodium phosphate buffer until processed for immunohistochemistry and immunofluorescence staining.

All protocols for immunolabeling of molecular markers followed a series of well standardized steps. After quenching endogenous peroxidase activity (3% H_2O_2, 10% methanol in buffer solution), free floating sections were incubated in a buffer solution containing 5% of blocking serum for 2 hours and then incubated for a minimum of 24 hours in one of the antibody solutions listed in table 3. To reveal the antigen-antibody binding, sections were incubated in a new antibody solution containing buffer and one of the secondary antibodies (fluorescent labelled or biotinylated) listed in Table 4.

Table 3: list of primary antibodies used in immunohistochemistry (IHC) and immunofluorescence (IF).

Antibody	*Host species*	*Target species*	*Supplier*	*Application*	*Paper*
Choline acetyltransferase	Goat	Mouse	Merck	IF	IV
Cre-recombinase (2D8)	Mouse	Mouse	Merck	IF	IV
Cre-recombinase (D7L7L)	Rabbit	Mouse	Cell Signaling	IHC	IV
D1R	Guinea pig	Mouse/Rat	Frontier Inst.	IF	II
DARPP-32	Rabbit	Mouse	Cell Signaling	IHC	IV
mGluR5	Rabbit	Mouse/Rat	Millipore	IF	II
Phospho-p44/p42 $MAPK^{Thr202/Tyr204}$ (pERK)	Rabbit	Mouse/Rat	Cell Signaling	IHC/IF	I,II,IV
Phospho-PKA-Ser/Thr	Rabbit	Mouse	Cell Signaling	IF	IV
Red Fluorescent Protein (RFP)	Mouse	Mouse	Abcam	IHC/IF	I
TO-PRO3	-	-	Invitrogen	IF	I
Tyrosine hydroxilase (TH)	Rabbit	Mouse/Rat	Pel-Freez	IHC	I,II, III, IV

Table 4: list of secondary antibodies used in immunohistochemistry (IHC) and immunofluorescence (IF).

Antibody	*Host species*	*Target species*	*Supplier*	*Application*	*Paper*
Alexa488 anti rabbit	Donkey	Mouse	Jackson Laboratory	IF	I, IV
BA1000 anti rabbit	Goat	Mouse/Rat	Vector Laboratories	IHC	I,II,III, IV
Cy3 anti mouse	Donkey	Mouse	Jackson Laboratory	IF	I, IV
Cy5 anti goat	Donkey	Mouse	Jackson Laboratory	IF	IV

Tissue preparation and D2R autoradiography

In Paper IV, an estimation of the levels of D2R protein was determined using a radioligand binding essay on striatal tissue of mice with different levels of Drd2 gene expression. Brains were rapidly extracted and transferred in dry ice-cold 2-methyl butane (Sigma-Aldrich) to frozen. Coronal sections (16 μm thickness) were cut serially through the antero-caudal striatum (Bregma +1.18 mm to -0.58 mm) using a cryostat and then mounted onto adhesive glass slides (SuperFrost Plus; Menzel Glaze, Braunschweig, Germany) and stored at -20 °C. Glass slides were prewashed with 50 mM Tris-HCl buffer (containing 120 mM NaCl, 5 mM KCl, 2mM CaCl2 and 1 mM MgCl2; pH 7,4) for 20 minutes at room temperature and then incubated in a buffer containing 4 nM of the radioactive D2/D3 ligand [3^H] raclopride (76 Ci/mmol) for 1 hour. After the incubation period, slides were rapidly rinsed in cold buffer and distilled water, airdried, and finally exposed to Kodak BioMax MR films with tritium standards for 10 weeks. Films were digitalized using a scanning machine (hp scanjet) and the ligand-binding intensity quantified with an optical density (O.D.) analysis.

Image analysis and quantification

Image analyses were performed using the open-source image processing program FIJI. Pictures from DAB (3,3'-diaminobenzidine) stained striatal sections were acquired using the Nikon DMS 1200F video camera mounted on a Nikon Eclipse 80i microscope (4X and 20X objective). For immunofluorescence staining, photomicrographs were acquired using the confocal Zeiss LSM710 NLO microscope (20X objective, in water immersion; 40X objective, in oil immersion). Co-localization of multiple fluorescent markers were confirmed using a Z-stack configuration.

In Papers I, II and IV, the number of immunoreactive cells was counted in an automated fashion using the “analyse particle” plugin offered by the software. Briefly, pictures were first converted into 8-bit grey scale and then into binary pictures by setting a threshold value that allowed to separate the objects of interest

apart from the background. In Papers I and IV, the extension of the viral transduction was calculated by subtracting the area without signal (mCherry, EGFP, and Cre negative) from the total striatal area.

Statistical analysis

Statistical analyses were performed using different versions of Prism GraphPad software. Data were analysed using factorial or repeated analysis of variance (ANOVA) followed by post hoc Bonferroni's multiple comparison test or Tukey´s test, as appropriate. When compared between groups on single sessions or time points, AIMs and dystonia ratings were analysed using non-parametric statistics followed by Dunn´s test correcting for multiple comparisons. For two-groups comparisons, paired or unpaired test were used when appropriate. Relations between variables were examined using the Pearson's r. Data were presented as group ± SEM (Papers I-IV) or as box plot and median, with whiskers annotating minimum and maximum values (Paper III and IV). The level of significance was set at $\alpha = 0.05$.

Results

Results

Paper I

Chemogenetic stimulation of striatal projection neurons modulates responses to Parkinson's disease therapy.

Classical theories hypothesize that direct and indirect SPNs are opposite modulators of movement initiation (Albin et al., 1989; Kravitz et al., 2010). In pathophysiological conditions, the same theories also implicate the hyperactivity of the indirect pathway in the development of PD motor symptoms, and the hyperactivity of the direct pathway in the genesis of LID (DeLong, 1990). These notions, however, were never subjected to direct experimental verification due to the lack of pharmacological approaches for cell-specific manipulation. To this end, the aim of the first study, was to address the relative contribution of striatal pathways to different motor behaviours using cell-type specific chemogenetic stimulation in a mouse model of PD and LID.

Validation of the chemogenetic approach in DA-intact mice

To validate the functionality of the DREADD approach, 4 weeks after receiving intrastriatal injections with the G_q-DREADD vector Cre-transgenic mice were sacrificed on CNO or vehicle. CNO induced pERK expression only in the AAV-transduced SPNs while no positive staining was detected in the absence of the ligand (vehicle condition), confirming the efficacy of the DREADD approach (see Figure 4).

In-vivo, the selective activation of direct and indirect pathway resulted in different modulation of motor behaviour. DA-intact mice expressing Cre in either SPN populations (D1-Cre for dSPNs and A2a-Cre for iSPNs) were infected into the right dorsolateral striatum with a Cre-inducible AAV coding for the expression of the stimulatory G_q-DREADD. After injection with the DREADD-selective ligand CNO or its vehicle, motor activity was recorded while mice were freely moving in an open field arena. Compared to baseline condition (vehicle), G_q-DREADD-mediated stimulation of iSPNs by CNO reduced both horizontal (distance travelled) and vertical activity (number of rearing events) in intact A2a-Cre mice. The opposite effect was observed in the D1-Cre mice, where the

activation of the dSPN by CNO increased the distance travelled, though not the number of rearing events. Furthermore, as the G_q-DREADD expressed unilaterally in the brain, both mouse lines showed a rotational bias upon CNO treatment: with iSPN-Cre mice preferentially leading towards the right injected side, and the dSPN-Cre mice rotating more towards the left side contralateral to the DREADD expression. These results supported the classical view that in normal physiological conditions dSPN and iSPN activity respectively promotes and inhibits movement initiation.

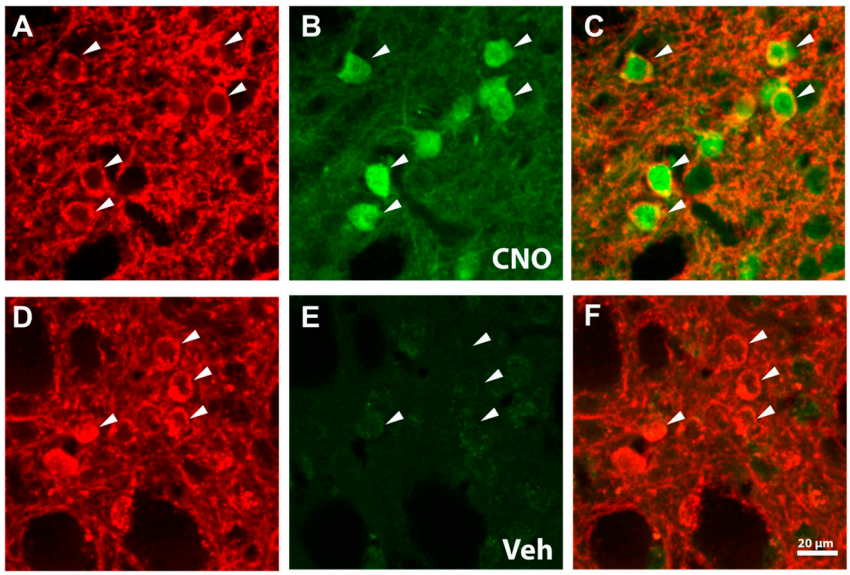

Figure 4: Histomolecular validation of Gq-DREADD. High magnification photomicrograph show mCherry expression in the soma and neuropile of transduced SPNs (indicated by the arrows) (A,D). Strong pERK immunoreactivy is only detected in the presence of the DREADD ligand CNO (B) in the trasduced cells (C) while basal levels are observed after vehicle treatment (E,F). Scale bar 20 µm. Extracted from Figure 1 of *Alcacer et al., 2017* (Paper I).

DREADD modulation of motor behaviour in a mouse model of PD

Next, we applied the same chemogenetic stimulation to Cre-trangenic mice which were previously rendered parkinsonian though the injection of 6-OHDA in the right nigro-striatal DA pathway. As observed in intact mice, G_q-DREADD activation of the indirect pathway strongly decrease whole-body movements in the open field test; aggravating even further the hypokinetic behaviour induced by the lesion. Opposite effect was mediated by the G_q-DREADD-dSPN stimulation, where treatment with CNO ameliorated the parkinsonian motor symptoms, as indicated by a significant increase in distance travelled and rearing events, and a

decrease of rotational bias; causal effect of the unilaterally DA-denervated striatum (see Figure 5).

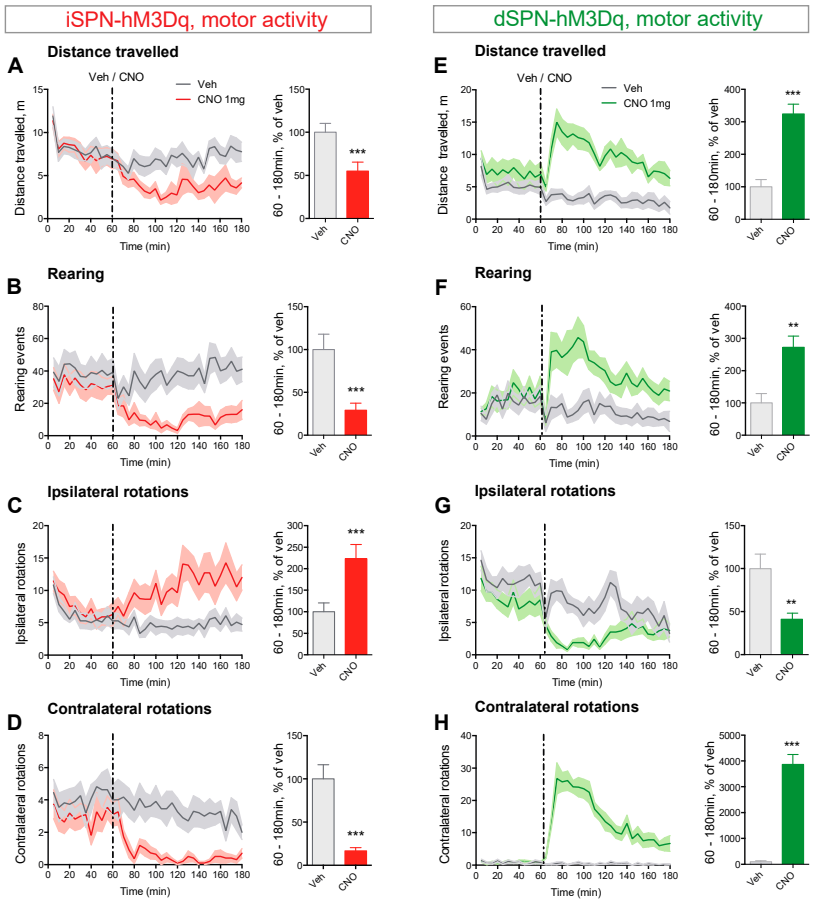

Figure 5: General motor behaviors observed upon Gq-DREADD-mediated stimulation of iSPNs or dSPNs in 6-OHDA-lesioned mice. Data were recorded in an open field set up from A2a-Cre or D1-Cre (E,H) mice transduced with the Gq-DREADD construct before and after the injection of CNO/vehicle (injection point is indicated by the dashed vertical line). Comparisons of distance travelled (A,E), rearings (B,F), ipsilateral rotations (C,G) and contralateral rotations (D,H) are represented for the entire test suration within each timecourse while bar diagrams represent recordings made from 60 to 180 minutes. Data are expressed as mean + SEM from A2a-Cre mice (n = 11) and D1-Cre mice (n = 10). Paired Student's t test: **P < 0.01; ***P < 0.001 for CNO vs. vehicle. Extracted from Figure 3 of *Alcacer et al., 2017* (Paper I).

Gq-DREADD-dSPN stimulation mimics the therapeutic effect of L-DOPA in a test of spontaneous forelimb use

Hemiparkinsonian mice experience severe hypokinesia in the forelimb contralateral to the lesion; a symptom of reduced DA content in the brain that is ameliorate by therapeutic doses of L-DOPA.

Forelimb hypokinesia in both A2aCre and D1-Cre mice was quantified using the cylinder test, a well-validated test of spontaneous forelimb usage during vertical exploration (see material and methods section). Based on the open field results, we hypothesized that CNO stimulation alone would aggravate the forelimb deficit in iSPN-G_q-DREADD expressing mice, while possibly mimicking the therapeutic effect of L-DOPA when acting on dSPNs.

We found that, activation of iSPNs by CNO (1 mg/kg) did not worsen the already severe limb hypokinesia observed in A2a-Cre lesioned mice treated with vehicle. However, in line with our predictions, dSPN stimulation by CNO restored forelimb use asymmetry in D1-Cre mice, fully mimicking the therapeutic effect of L-DOPA.

Finally, we looked at the effect of CNO when administered together with L-DOPA. This time, CNO produced a strong behavioural response in A2a-Cre mice, preventing the beneficial effect of L-DOPA, while D1-Cre animals were further biased toward a preferential use of the contralateral forelimb.

iSPN and dSPN Gq-DREADD stimulation oppositely modulate the dyskinetic effect of L-DOPA

DA-depleted A2a-Cre and D1-Cre mice were rendered dyskinetic with sub-chronic treatments of L-DOPA at escalating doses (1, 3, and 12 mg/kg). Next, CNO and L-DOPA were administered together in the attempt to modulate the already established dyskinesia. Once again, G_q-DREADD stimulation of either SPNs revealed opposing effects on the resulting behaviour. Briefly, G_q-DREADD-mediated activation of iSPN significantly reduced LID severity, while aggravating dyskinesia when increasing dSPNs activity. These effects were observed on all L-DOPA doses tested.

Gs-DREADD-dSPN-mediated activity unveils D1R signalling-dependent dyskinesias

In the second part of the study, we investigate the signalling pathways involved in the aberrant dSPNs activity and related dyskinetic behaviour. To this end, we exploit the DREADDs technology and use the G_q-DREADD or the G_s-DREADD constructs to selectively stimulate dSPNs of 6-OHDA-D1-Cre drug naïve mice. While the G_q-DREADD increases dSPN excitability via PLC activation, the G_s-

DREADD construct works by recruiting the same D1R signalling machinery. Mice from both groups were treated chronically with increasing doses of CNO (1,2,5 mg/kg) and rated for dyskinesia.

G_q-DREADD transduced mice developed mild-severity dyskinesias that were dose dependent and mainly represented by the orofacial component, while axial and limb AIMs were low or absent. On the contrary, G_s-DREADD dependent dSPNs stimulation induced appreciable levels of all AIM subtypes with severity comparable to those induced by a standard dyskinesogenic dose of L-DOPA (3 mg/kg) (see Figure 6).

To investigate further the signalling pathways recruited by the different DREADD constructs, we looked at two well-established molecular markers of dyskinesia, pERK and pPKA. Quantification of immunoreactive cells in the transduced dorsolateral striatum was performed at two time points post CNO injection: 30 and 140 minutes, corresponding to the peak and fading phase of dyskinesia scores, respectively. At both time points, the number of pERK and pPKA positive neurons was larger with the G_s-DREADD compared to the Gq-DREADD, correlating with the difference in dyskinesia observed with the two DREADD constructs.

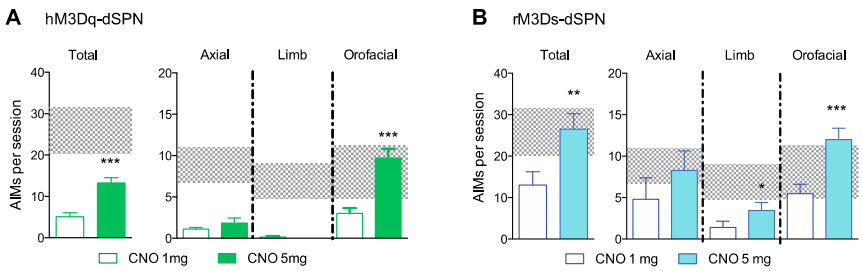

Figure 6: Gq- and Gs-DREADD-dependent dSPN activation results in different types and severity of dyskinetic behaviors in 6-OHDA-lesioned mice. Bar diagrams show the total AIM scores per session and separate axial, limb and orofacial scores following treatments with escalating doses of CNO (1 and 5 mg/kg) in Gq-DREADD (A) and Gs-DREADD-transduced mice (B). Grey-shaded area represenet the range (MEAN±SEM) of AIM scores induced by L-DOPA 3 mg/kg dose. Data are shown as mean + SEM from n = 7 mice transduced with hM3Dq and n = 8 mice transduced with rM3Ds. Paired Student's t test: *P < 0.05; **P < 0.01; ***P < 0.001 for CNO 5 mg/kg vs. CNO 1 mg/kg. Extracted from Figure 6 of *Alcacer et al., 2017* (Paper I).

Electrophysiological response to CNO in DREADD-transduced dSPN

To investigate further the different impact of G_q-DREADD versus G_s-DREADD stimulation on the striatal direct pathway neurons, we performed ex vivo electrophysiological recordings from transduced dSPN in corticostriatal slices. In striatal neurons transduced with either construct, bath application of CNO (10 µM) increased the generation of AP in response to brief current pulses but did not evoke AP *per se*. G_q-DREADD ability to drive AP did not differ between DA-intact and DA-depleted dSPNs. On the contrary, in slices obtained from G_s-

DREADD transduced mice, the effect of CNO was significantly higher in the absence of DA.

Severe dyskinesia requires Gs-DREADD-mediated dSPN activity and D2R pharmacological stimulation

As L-DOPA acts on both D1R and D2R, we asked whether the combination of G_s-DREADD expression in the dSPNs and the pharmacological stimulation of the D2Rs would further elevate the prodiskinetic properties of CNO. Indeed, combined treatment with CNO and quinpirole, a partial D2R agonist, induced AIMs severity scores that greatly exceeded those produced by very high doses of L-DOPA (12 mg/kg) (see Figure 7). This synergistic effect was observed in all three AIMs components, axial, limb and orofacial.

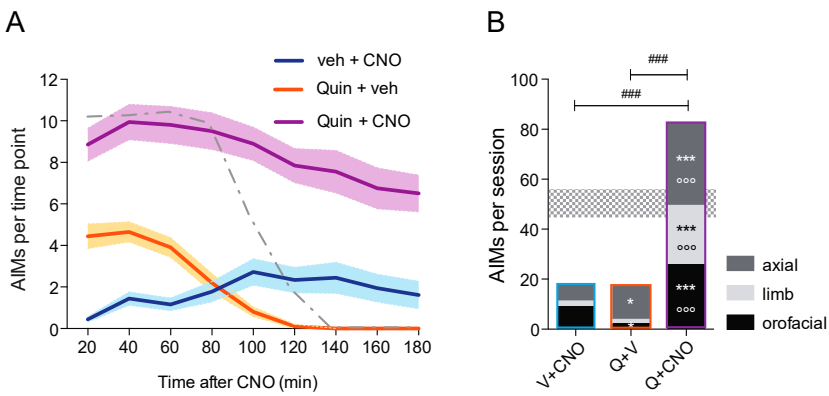

Figure 7: Combined Gs-DREADD-dSPN stimulation with D2 agonist treatment induces severe dyskinesia in 6-OHDA-lesioned mice. Different time curves representing AIMs severity scores induced by treatments with either CNO, the D2 agonist quinpirole (Quin) or a combination of both are compared to dyskinesia levels induced by 12 mg/kg L-DOPA (A). Bar diagrams show the sum of AIM scores per session, where axial, limb and orofacial values are represented with sub-bars. The grey shaded are represent the range (MEAN ± SEM) of AIM scores induced by 12 mg/kg L-DOPA (B). Tukey's post hoc test (n=9): ###P < 0.001 for Q+CNO vs. the indicated treatments. Individual AIM subtypes: *P < 0.05; ***P < 0.001 vs. V+CNO; °°°P < 0.001 vs. Q+V. Extracted from Figure 7 of *Alcacer et al., 2017* (Paper I).

Summary of Paper I

The results of this study revealed that the two striatal output pathways bidirectionally control both hypokinetic and dyskinetic motor abnormalities. Specifically, iSPN stimulation promotes hypokinesia and inhibits the prodyskinetic action of L-DOPA, while dSPN stimulation has opposite effects. Importantly, our results show that an engagement of both pathways is necessary to replicate the full spectrum and severity of L-DOPA-induced dyskinesia.

Paper II

D1-mGlu5 heteromers mediate noncanonical dopamine signal in Parkinson´s disease.

In this article we investigate the functional interaction between DA D1R and the metabotropic mGluR5 as a possible therapeutic target in the treatment of LID. The study present in Paper II is the result of the task force work of three distinct research groups. For the purpose of this thesis, I will only cover the part of the study addressed here in Lund.

D1R-mGluR5 heteromers increase in the DA-denervated striatum

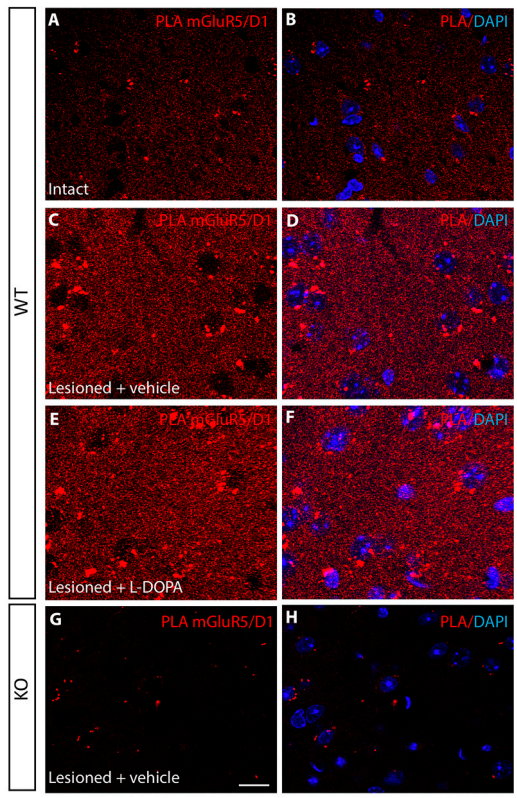

To search for D1R-mGluR5 complexes, tissue from DA-denervated and DA-intact striatum of WT and transgenic mGluR5^{KO-D1}mice was processed for protein ligation assay (PLA) with antibodies against both receptors. Fluorescence dots, representing the site of D1R-mGluR5 protein-protein interaction, were clearly detectable in the DA-denervated tissue of WT mice, and 2.5-fold more abundant than in the intact striatum. Fluorescent signal increased even further in dyskinetic mice treated chronically with L-DOPA. As expected, no clear signal was detected in transgenic mGluR5^{KO-D1}mice (see Figure 8).

Figure 8: Clusters of D1R-mGluR5 increases in the DA-denervated striatum of parkinsonian and dyskinetic mice. Red fluorescent lables dots show the site of protein-protein interaction between D1R and mGluR5 in the intact (A,B) and lesioned striatum of vehicle (C,D) and L-DOPA (6 mg/kg) treated mice (E,F). No clear fluorescent signal is detected in 6-OHDA-mice with a selective KO for the mGluR5 in the dSPNs (G,H). Nuclei were counterstained with DAPI (blue). Scale bar 10 µm. Extracted from Figure 6 of *Sebastianutto et al., 2020* (Paper II)

D1R-mGluR5 heteromers activate PLC signalling in the DA-denervated striatum

The second goal of the study was to investigate whether the physical interaction of the two receptors would also reflect into a D1R-dependent activation of PLC signaling. When DA levels are normal in the striatum, mGluR5 and D1R couple to different G-proteins resulting in the activation of separate signalling cascades: mGluR5 activity leads to phosphoinositide (PI) hydrolysis via PLCβ while D1R does not.

We measured the production of 3H-InsP as estimation of PLC activity and found that 3H-InsP levels increased in striatal tissue of 6-OHDA-lesioned rats incubated with the D1R agonist SKF38393 compared to basal conditions (vehicle). The greatest effect was however achieved by concomitant stimulation of D1R and mGluR5 when SKF38393 was applied together with the mGluR1/5 agonist DHPG. Finally, coincubation with the mGluR5 antagonist MTEP blocked DHPG-induced 3H-InsP while failed to reduce 3H-InsP mediated by SKF38393. So far, our data demonstrate that the physical interaction of the receptors reflects the synergistic activation of PLC signalling.

D1Rs and mGluR5s interact to induce ERK activation in the DA-denervated striatum

Increase of active ERK in the lesioned striatum reflects the aberrant D1R-mGluR5-dependend signalling in dyskinesia. Thus, in the second part of the study we investigate the effect of PLC inhibition on pERK levels induced by L-DOPA or SKF38393 in both rats and mice with 6-OHDA MFB lesions. Treatments with L-DOPA (6 mg/kg) and SKF38393 (2/6 mg/kg) produced a large increase of pERK in both rat and mouse DA-denervated striatum. This increase was effectively reduced in animals preventively administered with the PLC inhibitor U73122 (30 mg/kg). When $mGluR5^{KO\text{-}D1}$ mice were treated with SKF38393 pERK signal was dimmed to level comparable to those observed in WT mice treated with the combination of D1R agonists and PLC inhibitor U73122 (see Figure 9).

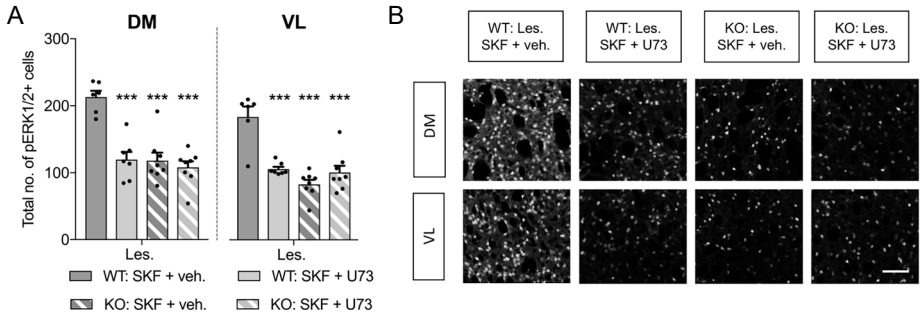

Figure 9: mGluR5 KO attenuates D1R-dependent pERK in the DA-depleted striatum. Bargraph show the number of pERK positive cells induced by SKF38393 and SKF38393 + PLC inhibitor U73122 in the DA-lesion dorsomedial (DM) and ventrolateral (VL) striatum of WT (n=6-8) and mGluR5KO-D1 (n=6/8) mice (A). Bonferroni´s test: *** $P < 0.001$ vs WT:SKF+vehicle. Photomicrographs show representative pERK stainings for the two genotypes (WT and mGluR5KO-D1) and each of the four treatment conditions. Scale bar 200 µm. Extracted from Figure 7 of *Sebastianutto et al., 2020* (Paper II)

PLC inhibition reduces D1R-mediated and L-DOPA induced dyskinesia

In the last part of the study, we set out to verify the antidiskinetic effect of both MTEP and PLC inhibitor in 6-OHDA-lesioned WT mice and mice with reduced levels of expression for mGluR5 (mGluR5^{KD-D1}). Mice from both genotypes were rated for dyskinesia severity after treatment with L-DOPA, SKF38393 and quinpirole, a D2 receptor agonist. Peak severity of dyskinesia was significantly reduced by MTEP or PLC inhibitor when administered in combination with L-DOPA or SKF38393 in WT mice. Similarly, mGluR^{KD-D1} mice having an almost complete loss of mGluR5 expression in the dSPNs, developed milder dyskinesias when challenged with the same DA agonists. Differently from the effect observed in the WT control group, AIMs severity was not ameliorated by MTEP or by the PLC inhibitor U73122 in mGluR5^{KD-D1} mice. Finally, quinpirole-induced dyskinesia was as severe in mGluR5^{KD-D1} mice as in WT controls and did not change in severity and duration when administered together with MTEP or U73122.

Summary of Paper II

The results obtained from Paper II reveal that, D1R and mGluR5 form heteromers in dSPNs in rodent models of PD. These receptor re-arrangements mediate maladaptive molecular changes associated with the development of LID. Moreover, we show that pharmacological antagonism of mGluR5 does not improve LID in mice with conditional ablation of mGluR5 in dSPNs, thus shedding light on the mechanisms of action of antidyskinetic treatments targeting mGluR5.

Paper III

Distinct pattern of dyskinetic and dystonic features following D1 or D2 receptor stimulation in a mouse model of parkinsonism.

In Paper I and Paper II we showed how the sole activation of dSPNs can induce dyskinesia in a mouse model of PD and how the maladaptive changes associated to D1R signalling pathways mediate this behaviour. However, an accurate analysis of D1R-dependent dyskinesias, suggested that a synergistic involvement of both D1Rs and D2Rs is important to fully replicate the complex palette of abnormal behaviours that is characteristic of LID. To elucidate the dyskinetic potentials behind D1R and D2R stimulation, we set out to compare patterns of dyskinetic and dystonic behaviours induced by the systemic administration of agonists selective for either receptors or both, in drug naïve mice with unilateral 6-OHDA lesion.

D1 and D2 receptors control different features of dyskinesia

Mice with unilateral 6-OHDA lesion in the right MFB were randomly divided in four groups to receive a chronic course of one of the following DA agonists: the partial D1 agonist SKF38393 (3 and 6 mg/kg), the D2/D3 agonist quinpirole (0.5 and 1 mg/kg), the selective D2 agonist sumanirole (2 and 4 mg/kg) and L-DOPA (3 and 6 mg/kg). Dyskinetic behaviours developed for all four treatment conditions. Peak severity scores (20-60 minutes) did not differ between selective DA-agonist treatments but overall, L-DOPA had the more severe dyskinetic effect.

A separate analysis of the three dyskinesia subtypes revealed that selective D1R or D2R stimulation induced different types of dyskinesia. Specifically, treatment with the D1R agonist SKF38393 induced prominent limb and orofacial AIMs, while axial AIMs were mild or absent. The inverse pattern was observed after treatment with the D2-class agonist quinpirole and sumanirole, where over 70% of the total dyskinesia scores was represented by the axial subtype.

Development of a new rating scale to assess dystonic behaviours in a mouse model of LID

Dystonia severity scores were assigned to different body segments as described in Table 5 and represented in Figure 10 and based on a time-based grading scale (see methods section of this thesis).

Table 5: Classification and detail description of the dystonic features included in the scale

Dystonic features	*Criterion*	*Description*
Trunk/neck dystonia (Tr/ne)	Sustained deviation of the head from the body axis.	The head is pulled towards the side contralateral to the lesion because of lateral flexion/torsion of neck and upper trunk. The dystonic feature is interrupted when the head is pulled back to a normal position.
Contralateral forelimb dystonia (cFL)	Sustained stretching of the forelimb in a non-weight-bearing position	Sustained shoulder adduction and elbow extension; the forelimb is kept extended underneath the body when the animal turns. The dystonic feature is interrupted when the elbow bends and the palm touches the floor to sustain the animal´s body.
Ipsilateral forelimb dystonia (iFL)	Sustained deviation of the forelimb from the body axis.	Sustained shoulder extension (often combined with abduction) and elbow extension; the forelimb is pulled sideward or backward. The dystonic feature is interrupted when the elbow bends and the palm touches the floor to sustain the animal´s body.
Contralateral hindlimb dystonia (cHL)	Sustained inward deviation of the hindlimb relative to the body axis.	The hindlimb is adducted at the hip joint and extended at knee and/or ankle joints; the hindlimb is dragged under the body while the animal rotates. The dystonic feature is interrupted when the hindlimb goes back to a normal position.
Ipsilateral hindlimb dystonia (iHL)	Sustained outward deviation of the hindlimb relative to the body axis.	The hindlimb is abducted at the hip joint and extended at knee and/or ankle joints. The dystonic feature is interrupted when the limb goes back to a normal position.
Straub tail (Tail)	Stiff erected, tail markedly lifted from the floor	Sustained dorsiflexion of the tail starting from its base. The tail may assume a curved S-shape or exhibit slow, up-and-down or lateral movements. The dystonic feature is interrupted when the tail is pulled back to the floor.

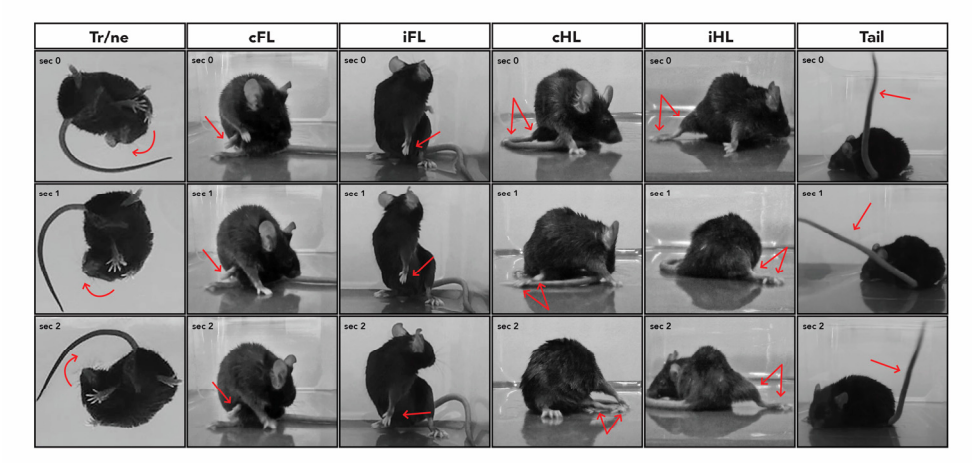

Figure 10: Video frames illustrating the dystonic features reported in Table 5. Half-scores from 0-3 are applied to each of the six topographic dystonic subtyes. Extracted from *Andreoli et al., 2021* (Paper III), Figure 2.

Dystonia scores correlate with geometric measures of altered postures

To the best of our knowledge, this is first rating scale that allows for assessing dystonic features in a mouse model of LID. Considering the novelty of the approach, we decided to validate some of the dystonic features included in the scale with geometric correlates that allowed for an independent verification of the observed behaviours.

We found that tr/ne dystonia correlated with the angle ("axial bending angle") generated from the intersection of two vectors: one extending between hindpaws and the other one connecting the nose to the base of the tail. Small degrees of axial bending angle strongly correlated with severe tr/ne dystonia.

Similarly, hindlimb dystonia was correlated to the angle formed between the intersection of two vectors reflecting the position of left and right hindpaws on the floor ("hindpaw angle"). Wide angles correlated to high degree divergence between the hindlimbs, and therefore to severe dystonia (see cHL and iHL description in Table 5).

D2R agonists induce dystonic forms of dyskinesia in a mouse model of PD

In the second part of Paper III, drug-induced behaviours were rated using the novel scale to dissect the different contribution of D1R and D2R stimulation in the development of dystonic features of LID.

At peak-drug effect (20-60 minutes post injection) agonists targeting D2R, quinpirole and sumanirole, induced significantly more dystonia than the D1R agonist SKF38383. Dystonic features affecting or pointing towards the side of the

body contralateral to the lesion such (tr/ne, cFL and cHL) had similar severity in mice treated with the D2R agonists or L-DOPA, while the effect on the ipsilateral side was mainly under control of the most selective D2R agonist (sumanirole). The only appreciable dystonic feature associated with SKF38393 treatment was the Straub tail phenomenon (see Figure 11).

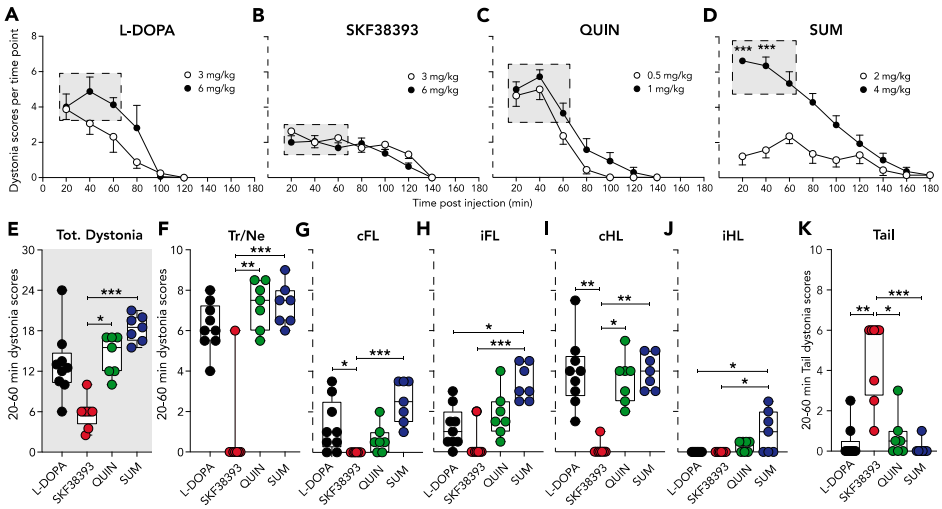

Figure 11: Severity of dystonic features induced by different dopaminergic treatments. When the four dopaminergic treatments were administered at the highest dose, dystonia severity scores always peaked between 20 and 60 minutes post injection (as highlighted by the grey shaded area) (A). Data are showed as MEAN± SEM. Post hoc Bonferroni´s test: *** P < 0.001. Box and whiskers diagrams show the sum of dystonia scores at peak drug effect (E) and separate scores for tr/ne (F), cFL (G), iFL (H), cHL (I), iHL (J) and Tail (K) following treatments with L-DOPA (n=9), SKF38393 (n=8), quinpirole (QUIN, n=7) and sumanirole (SUM, n=7). Dunn´s post hoc test: * P< 0.05; **P < 0.01; *** P < 0.001 in the indicated comparisons. Extracted from *Andreoli et al., 2021* (Paper III), Figure 3.

Distinct patterns of open field motion upon D1R or D2R stimulation

Different agonist treatments resulted in different patterns of motion in the open field arena. Specifically, mice treated with SKF38393 showed greater distance travelled and speed compared to vehicle, L-DOPA and sumanirole treated mice. Moreover, SKF38393 treated mice were able to explore the entire surface of the arena whereas horizontal locomotion was severely affected in sumanirole treated mice, as they remained confined to one quadrant of the arena (see Figure 12).

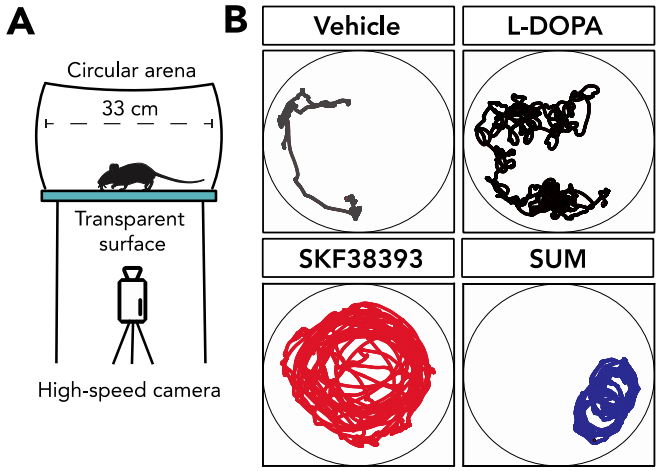

Figure 12: Distinctive motion patterns observed in the open field arena in 6-OHDA-mice after treatments with selective D1R and D2R receptor agonists and L-DOPA. Drawing representing the recording setup (A). Traces representative of the animal movement pattern inside the circular arena (B). Extracted from Figure 6 of *Andreoli et al., 2021* (Paper III).

Effect of DAR antagonists on dyskinesia and dystonia

In the last part of the study, we confirmed the different involvement of D1R and D2R in generating hyperkinetic versus dystonic components of LID by using a combination of selective DAR antagonists and L-DOPA. SCH23390, a D1/5R antagonist greatly reduced limb and orofacial dyskinesia but did not affect the severity of axial dyskinesia and L-DOPA-induced dystonia. On the contrary, the D2R antagonist L741626 had a greater impact in alleviating axial dyskinesia compared to the limb and orofacial AIM subtype and had a beneficial effect on most severe dystonic features induced by L-DOPA (tr/ne and cHL).

Summary of Paper III

This study presents an extensive comparison of dyskinetic movements and dystonic postures induced by different DA agonists in a unilateral mouse model of PD. First, we show how pharmacological stimulation of either D1R or D2R mediates different aspects of dyskinetic behavior. Second, we introduce and validate a new rating scale for the evaluation of the dystonic behavior in a mouse model of LID. In conclusion, the main finding of this study is that drugs acting on the D1R elicit mainly hyperkinetic forms of dyskinesia, while D2R agonists preferentially mediate its slow and dystonic features.

Paper IV

Pivotal role of indirect pathway-D2 receptors in parkinsonian and dyskinetic states.

In Paper III, we demonstrated that pharmacological stimulation of D2R plays a key role in both dyskinesia and dystonia. However, the study was limited to a pure pharmacological study design that did not allow to discern between the contribution of D2Rs that are expressed in different cell types and regions of the brain. Therefore, in this fourth Paper, we focused on the striatal D2Rs expressed in the iSPNs and we present an extensive behavioral study in two mouse models of iSPN-selective D2R ablation. The impact of the cell type specific receptor ablation was examined in both normal and pathophysiological states of PD, dyskinesia, and dystonia.

Generation of a new D2R knock-out mouse

An iSPNs selective ablation of the *Drd2* gene was achieved with the delivery of an *ad hoc* designed Cre-expressing and PPA promoter-dependent AAV vector into the dorsolateral striatum of homozygous *Drd2*$^{loxp/loxP}$ mice. The AAV injection was confined to right striatum, to generate a mouse with a unilateral KO for the receptor (AAV-Drd2KO mice).

We compared the cell type specificity and the efficacy of the D2R loss of our model with another well-validated and largely used constitutive D2RKO mouse model (bilateral KO model; D2RKO$^{-/-}$ as in (Lemos et al., 2016)). An O.D analysis performed on films exposed to radioactive raclopride [H3] showed ~75% reduction of binding efficacy to the D2R in the right striatum of AAV-Drd2KO mice compared to the control condition (WT mice injected with the same AAV construct; AAV-Drd2WT mice). A similar degree of D2R reduction (~80-85%) was observed also in the striatum of D2RKO$^{-/-}$ mice. From the histological analysis, we found that the viral approach let to a highly specific Cre expression in the iSPNs, with less than 0.1% of CINs and less than 10% of dSPNs transduced by the virus (see Figure 13).

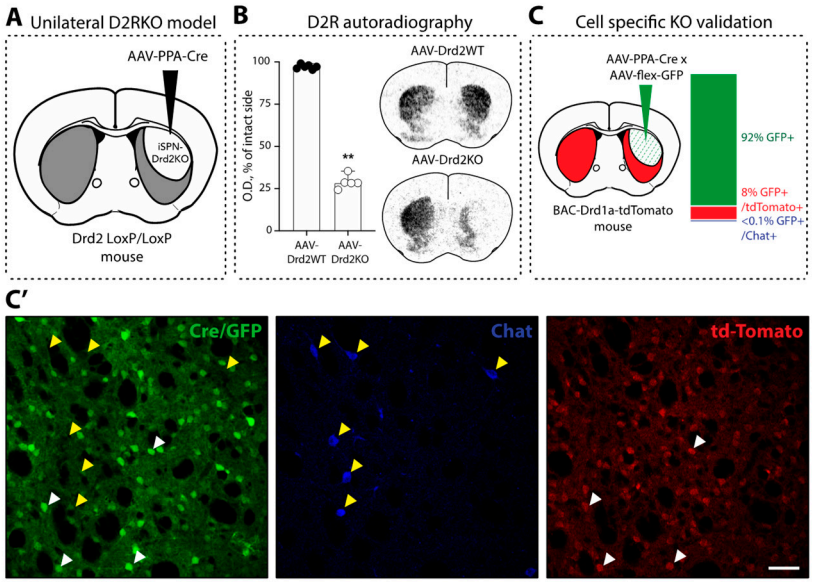

Figure 13: Histological validation of the viral mediated iSPN-D2RKO model. Graphic representation of the viral-mediated and iSPN-specific D2RKO approach (A). O.D. analysis show the percentage of reduction of radioactive raclopride [H3] to the D2Rs in the right striatum of Drd2loxP/loxP mice injected with the AAV-PPA-Cre construct (AAV-Drd2KO mice) respect to the control WT mice (AAV-Drd2WT mice) (B). Number of Cre expressing cells were quantified in coronal striatal sections having fluorescent lables for dSPNs and ChAT positive interneurons (CIN) (C). High magnification photographs show no colocalization of markers for Cre (GFP; greeen) and ChAT (blue) expressing neurons (yellow arrows) and sparse colabelling of Cre signal and tdTomato positive dSPNs (white arrows)(C′). Scale bar 50 µm. Extracted from *Andreoli et al., unpublished manuscript* (Paper IV), Figure 1.

Impact of iSPN-D2R ablation on the motor behaviour of DA-intact mice

Patterns of open field motions were analysed in DA-intact mice having normal (WT control) or altered iSPN-D2R expression. The latter were obtained with two different approaches: bilateral D2RKO mice ($Drd2KO^{-/+}$ and $Drd2KO^{-/-}$), generated from the crossing of $Drd2^{loxP/loxP}$ and A2a-Cre transgenic mice, and mice with unilateral D2RKO, obtained with the AAV-mediated strategy (as explained in the previous section).

In the bilateral model, mice with severe reduction of D2R levels ($Drd2KO^{-/-}$) displayed severe akinesia and hypokinesia, as compared to WT mice they were immobile for about half of the time and showed reduced speed and exploratory behaviour in the open field arena. On the contrary, animals that still presented ~50% of the receptor ($Drd2KO^{-/+}$) were only significantly affected in the amount of distance travelled. Interestingly, depletion of D2Rs targeting the dorsolateral striatum in one side of the brain (AAV-Drd2KO) did not decrease the general motor behaviour but induced a strong ipsilateral rotational bias and compromised the ipsilateral forelimb performance in the cylinder test.

Impact of iSPN-D2R ablation on the motor behaviour of 6-OHDA-lesioned mice

Next, WT control and D2RKO mice obtained from both strategies underwent unilateral injection of 6-OHDA in the right nigro-striatal pathway and were tested again in the open field three weeks post lesion. As the loss of DA content in the striatum is associate to reduced motor performances in the unilateral mouse model of PD, we hypothesized that the effect of the lesion would be exacerbated in mice lacking the expression of D2Rs in the iSPNs. Surprisingly, the results obtained from the open field analysis showed that impact of the DA lesion had less severe effects in D2R deficient mice. This paradoxical response was confirmed in both bilaterally and unilaterally D2R depleted mice. Moreover, we found that the combination of lack of DA stimulation and absence of D2Rs in the iSPNs affected the pattern of exploration inside the arena. Indeed, mice from both D2RKO strategies spent more time exploring the center of the arena; a region that is considered highly anxiogenic for the mouse.

Selective ablation of D2R from the iSPNs prevents D2R agonists-dependent dyskinesia and ameliorates LID

First, we addressed the role of iSPN-D2R in dyskinesia using the already established bilateral KO model. In line with the results obtained in Paper III, 6-OHDA-lesioned mice with normal D2R expression levels (WT controls) developed severe axial AIMs after single or repeated injections (5 days treatment) with D2R agonists quinpirole and sumanirole. D2R-dependent AIMs scores were halved in severity in $Drd2KO^{+/-}$ mice, while dyskinesia development was completely prevented in $Drd2KO^{-/-}$ mice. Total ALO scores were also significantly reduced in $Drd2KO^{-/-}$ mice after treatment with SKF38393 and L-DOPA.

Next, we administered the same DA agonist treatments to mice with DA-denervation and D2RKO on the right striatum. Preventing D2R activation on the iSPNs of the DA-depleted side was sufficient to fully counteract the development of quinpirole and sumanirole-induced dyskinesia. On the contrary, D1R-dependent dyskinesia was not affected in the unilateral KO model. AAV-Drd2KO mice displayed reduced dyskinesia severity when treated with L-DOPA. Importantly, a greater antidyskinetic effect was reported for the axial and limb components, while orofacial AIMs were less affected by the D2RKO during LID (see Figure 14).

All together these results demonstrate that: (i) D2R agonists treatments modulate their dyskinetic effect by interacting with D2R expressed in the iSPNs of the DA-depleted striatum; (ii) activation of iSPN-D2R is causal to the development of axial dyskinesia.

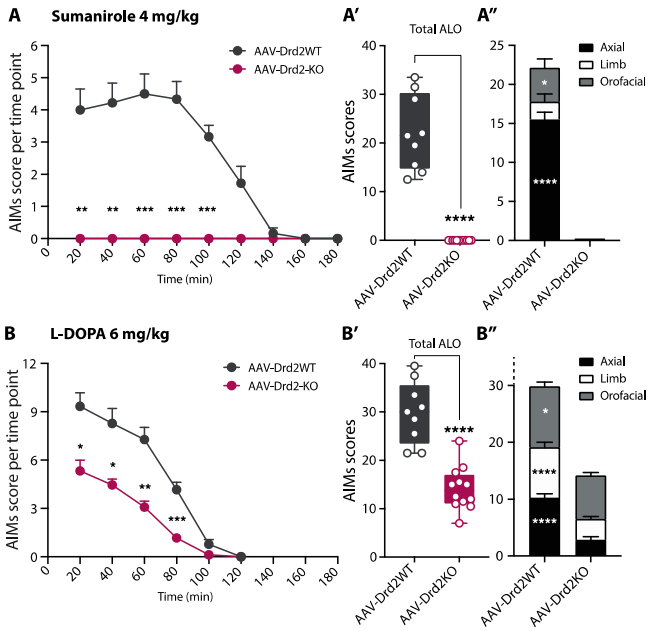

Figure 14: iSPN-D2Rs in the DA-denervated striatum modulate the dyskinetic response to treatments with D2-class agonists and L-DOPA. Time course of summed axial, limb and orofacial AIMs scores show the response in DA-depleted AAV-Drd2WT (n=9) and AAV-Drd2KO (n=12) mice to chronic treatments (day 5) with the D2R agonist sumanirole (4 mg/kg) and with the DAR agonist L-DOPA (6 mg/kg) (A, B). Data are displayed as MEAN± SEM. Bonferroni´s post hoc test: *P < 0.05; **P < 0.01; *** P < 0.001. Dyskinesias induced by sumanirole are prevented in mice unilaterally depletated from the iSPN-D2Rs (B´, B´´) and ameliorated in the same mice after treatment with L-DOPA (C´, C´´). Box and whiskers diagrams report the total ALO scores within 180 minutes observation period, whereas bar diagrams (MEAN ± SEM) show separated values for axial, limb and orofacial AIMs. Mann-Whitney test: **** P < 0.0001. Post hoc Bonferroni´s test: *P < 0.05; **** P < 0.0001. Extracted from Figure 7 of *Andreoli et al., unpublished manuscript* (Paper IV).

iSPN-D2Rs mediate dystonia in a mouse model of dyskinesia

We next asked whether the axial component would be the only dystonic feature of dyskinesia to be affected by the iSPN-specific D2R ablation. To this end, videos of dyskinetic mice from both bilateral and unilateral-AAV-mediated D2RKO groups (and the respective WT controls) were rated using the novel dystonia scale introduced in Paper III. All forms of dystonia were prevented in mice with any iSPN-D2RKO intervention when treated with sumanirole. Interestingly, tail dystonia, which is dependent on D1R stimulation was unaffected by the iSPN-D2RKO. Finally, we report that L-DOPA-induced dystonia was less severe in D2RKO mice, however, the positive effect was greater in the unilateral D2RKO model than in the bilateral D2RKO mice.

Loss of iSPN-D2Rs in the dorsolateral striatum modulates ERK activation in LID

In animal models of PD, the appearance of dyskinetic behavior has been correlated with aberrant pERK activity in the dSPNs of the lesioned striatum (Santini et al., 2009). Considering the significant improvement of LID severity obtained from the viral-mediated D2RKO approach, we looked at changes in ERK activity by counting pERK-immunoreactive cells from the dorsolateral striata of AAV-Drd2WT and AAV-Drd2KO mice treated with L-DOPA or vehicle.

To our surprise, absence of iSPN-D2R signalling in the striatum affected the levels of pERK induced by L-DOPA as demonstrated by the significant reduction in the number of positive cells in the AAV-Drd2KO mice compared to the AAV injected WT control mice. Whether the remaining pERK-positive cells belong to the dSPN or iSPN population is still under investigation. Negligible levels of pERK were detected in mice treated with vehicle from both genotypes (see Figure 15).

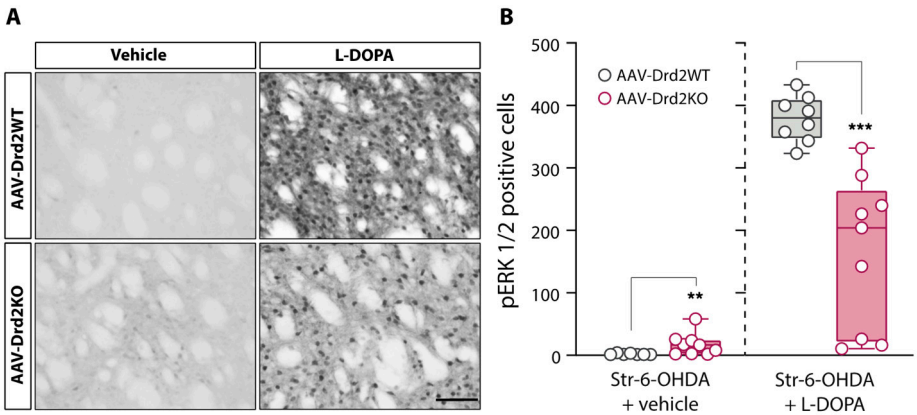

Figure 15: Loss of D2Rs in the lesioned dorso-lateral striatum modulates pERK expression after treatment with L-DOPA. High magnification photomicrographs (20x) of pERK stained striatal (Str) sections of AAV-Drd2WT (and AAV-Drd2KO after L-DOPA (3 mg/kg) or vehicle injection (A). Box and whiskers diagrams report the number of pERK positive cells averaged between three striatal levels with incresing rostro-caudality from bregma (B). n=7/8 AAV-Drd2WT, n=8/9 AAV-Drd2KO. Mann-Whitney test: **p<0.01 and ***p<0.001 as reported in the indicate comparisons (see horizontal lines). Extracted from Figure 9 of *Andreoli et al., unpublished manuscript* (Paper IV).

Summary of Paper IV

In DA-intact mice, genetic iSPN-D2R ablation can fully recapitulate the bradykinetic and hypokinetic aspects of PD only when both sides of the striatum are affected. Whereas, when restricted to one hemisphere, the receptor KO induces strong rotational bias and forelimb use deficit in intact mice. In both models of iSPN-D2R ablation, the development of LID and D2R-mediated dyskinesia are significantly reduced and completely prevented, respectively. Moreover, when applied to the 6-OHDA-lesioned side, iSPN-D2RKO partly counteracts the aberrant increase of ERK signalling activation induced by L-DOPA. Taken together, the results show that lower levels of D2R expression in iSPNs result in more severe parkinsonian features and less severe dyskinetic features, specifically ameliorating the dystonic components of LID.

Discussion

Discussion

dSPN and iSPN: a battle over movement control?

With an influential study published in 2010, Kravitz and collaborators showed that, in-vivo direct optogenetic dSPNs activation increases movement, while the same activation exerted on the iSPNs leads to the opposite outcome in the mouse. These data provided the first explicit experimental support to the classic go/no-go model of the BG pathways. However, when asking how DA modulates SPNs activity and the resulting motor behaviour, optogenetic stimulation might not be the right methodology for the question. In fact, light-activated ion-channels and DA do not affect neuronal activity in the same way. While optogenetic stimulation imposes artificial spiking patterns, DA on the contrary activates intracellular signalling pathways that only increase the neuronal response to incoming stimuli, making the cell more or less excitable depending on the type of DAR with which DA interacts.

In this context, the present thesis takes a step forward towards understanding how dSPN and iSPN activity contributes to different types of motor behaviour, using technologies that better mimic the physiological mechanisms regulated by DA, as the chemogenetic approach allowed us to mimic receptor-mediated changes in neuronal excitability.

In Paper I, G_q-DREADD stimulation of D1-Cre and A2aCre DA-intact mice was combined to open field recordings to monitor changes in the whole-body movement, while activating dSPNs and iSPNs respectively. In accordance with the go/no-go model (and with Kravitz and collaborators), we report that increased dSPN excitability led to an increase of general open field activity in D1-Cre mice, while the opposite effect was observed in the A2a-Cre line. Moreover, as the chemogenetic stimulation was applied unilaterally, both D1- and A2a-Cre mice experienced a strong rotational bias, in the direction contralateral or ipsilateral to the side of the DREADD stimulation, respectively. Interestingly, even when confined to one hemisphere, iSPNs stimulation via Gq-DREADD resulted in severe hypokinetic features in DA-intact mice. The relationship between iSPNs hyperactivity and parkinsonism in the mouse will be largely discussed in the next paragraph.

Different modulation of iSPN activity relates to different motor symptoms of PD

In PD, hypokinesia and bradykinesia are casually linked with the loss of DA content in the striatum, as the lack of D2R stimulation results in iSPN disinhibition

and therefore overactivity of the indirect pathway. Yet, up to this point neither optogenetic (Kravitz et al., 2010), nor the G_q-DREADD stimulation (addressed in Paper I) could empirically validate the above-mentioned hypothesis; as they both increase iSPNs excitability via mechanisms that are not related to the D2R. To fill this gap, the first aim of Paper IV was to investigate whether the targeted genetic ablation of iSPN-D2Rs would be sufficient to reproduce parkinsonism in DA-intact mice.

Previously published studies have shown how genetic D2Rs ablation in the mouse is sufficient to cause akinesia and bradykinesia (Bello et al., 2017; Kelly et al., 2008; Lemos et al., 2016). However, these studies are based on genetic KO strategies that either act globally in the brain, as they fail to target a specific cell population or brain structure, or activate during an early developmental state, with possible consequences on the neuronal circuitries dynamic.

To solve this methodological gap, Paper IV introduces a new D2RKO mouse model based on an AAV-mediated Cre/loxP strategy (AAV-Drd2KO mouse). The AAV strategy presents several advantages, as it is (i) highly selective for the iSPNs, (ii) injectable, and therefore confinable to anatomically distinct regions of the brain, (iii) suitable for the adult mouse brain.

When restricted to the dorsolateral striatum of one hemisphere, the selective iSPN-D2RKO was sufficient to induce a strong rotational bias towards the injected side. However, the same strategy failed to induce other parkinsonian-like behaviours that on the contrary were reported to occur after G_q-DREADD activation of iSPNs in Paper I, and in other constitutive D2RKO mouse models (Lemos et al., 2016) (one of which also investigated in Paper IV). The discrepancy between the results obtained from the G_q-DREADD stimulation and the AAV-mediated D2RKO might relate to the different signalling cascades involved in the process. Supposedly, both G_q-DREADD stimulation and D2RKO increase iSPNs activity. However, while the chemogenetic approach drives the cell towards more excitable states via increase of intracellular Ca^{2+} levels (G_q/PLC/PKC pathway), the receptor KO approach works via a disinhibition mechanism, as it blocks the action of DA towards the G_i-coupled D2R. Regarding the disagreement with other studies using conditional D2RKO models (Kelly et al., 2008; Lemos et al., 2016), we can speculate that this difference relates to the fact that with a conditional KO the gene exertion equally affects both sides of the brain. We cannot exclude that if applied on both striatal hemispheres, our AAV-mediated KO would result in a more pronounced parkinsonian phenotype. Indeed, already with the unilateral approach, AAV-Drd2KO mice displayed less, yet not significant, rearing events compared to the WT control. This trend of reduced vertical exploration was further confirmed in the cylinder test, where DA-intact and unilaterally D2R-depleted mice showed severe ipsilateral forelimb akinesia, one of the standard phenotypes of the 6-OHDA-lesioned model.

dSPN and D1R signalling pathways in dyskinesia

There is a large consensus that aberrant D1R stimulation is a key factor to the increase of dSPN activity during dyskinesia (Maltese et al., 2021; Parker et al., 2018). However, the molecular machinery that translates receptor stimulation to pathophysiological neuronal excitability is still a matter of debate. Paper I and Paper II address some of these questions.

In Paper I, we used chemogenetics to selectively stimulate striatal originating-direct pathway neurons in a mouse model of PD. Specifically, we took advantage of the variety of engineered GCPRs offered by the DREADD technology to investigate the role of two distinct molecular pathways in dyskinesia: the $G_{\alpha q}$- and $G_{\alpha s}$-related pathway. To target and activate the dSPN population in-vivo selectively, the gene expressing either DREADD receptors was inserted in the genome of D1-Cre transgenic mice via Cre-inducible AAV. When compared to the effect of a standard dose of L-DOPA (3 mg/kg), stimulation of G_q-DREADD in DA-depleted D1-Cre mice induced mild dyskinesia, mainly restricted to the orofacial region, and mild levels of pERK and pPKA. Conversely, Gs-DREADD stimulation of the same neuronal type produced more diverse and moderate dyskinesias, along with a larger and sustained pERK/pPKA activation. The latter results were in line with previous findings showing that pharmacological D1R stimulation in lesioned mice leads to dyskinesia and to an aberrant increase of ERK activity in the DA-depleted striatum (Darmopil et al., 2009; Santini et al., 2009; Westin et al., 2007).

Shortly after the publication of Paper I, Gomez and collaborators showed how following CNO administration in-vivo, it is clozapine, and not CNO, that crosses the BBB and activates the DREADDs (Gomez et al., 2017). The existence of a reverse metabolism that back-converts CNO to clozapine in-vivo it is strictly relevant for the reliability of our study. Indeed, clozapine may exert its activity on other endogenous non-DREADD targets and lead to confounding behavioural results. As clozapine can acts on both D1R and D2R (Tauscher et al., 2004), we tested the effect of CNO on dyskinesia in WT mice lacking the expression of the DREADD. These results, that however remained unpublished, showed no CNO effects in either the reduction or increase of LID.

In normal physiological conditions, D1R stimulation on its own does not activate ERK (Gerfen et al., 2002). This effect only occurs in the DA-denervated striatum, where D1R-mediated pERK is dependent on the crosstalk between the “canonical” cAMP/PKA/DARPP-32 D1R pathway and the Gαq-dependent mGluR5/PLC/PKC signalling cascade (Fieblinger et al., 2014b; Rylander et al., 2009). As a matter of fact, mGluR5 are of particular interest in the treatment of LID: the receptor expression increases in the DA-depleted striatum of dyskinetic rodents (Konradi et al., 2004; Ouattara et al., 2011) and pharmacological antagonism of mGluR5 can reduce both ERK activation and AIMs severity in LID (Fieblinger et al., 2014b). Based on these observations, we hypothesized that as

the number of glutamate receptors increases in the DA-depleted striatum, D1Rs may relocate in the lipidic membrane (Fiorentini et al., 2006) and form physical and functionally active heteromers with the mGluR5s. This hypothesis was investigated in Paper II.

In situ PLA analysis confirmed the existence of physical interaction between D1R and mGluR5 in the DA-depleted dSPNs. This interaction was largely increased in dyskinetic mice subjected to a chronic course of L-DOPA treatment, therefore suggesting that the formation of receptor complexes might be crucial to drive maladaptive intracellular signalling in LID. Through our ex-vivo analysis we identified the D1R-mGluR5-dependent activation of PLC as a promising target for the prevention of LID. This assumption was further confirmed in-vivo, where the pharmacological inhibition of PLC improved dyskinesia and reduced the striatal activation of ERK in mice treated with either L-DOPA or the D1R agonists SKF38393; yet, without interfering with the antiakinetic properties of these treatments.

Finally in Paper IV, the analysis performed on striatal sections of AAV-Drd2KO mice treated with L-DOPA revealed a marked reduction in the number of pERK immunoreactive cells compared to the WT control group. Regarding the already mentioned literature on pERK and the conclusions from Paper I and Paper II, these results are unexpected and will therefore require further histological validation. In fact, the current methodological approach is strictly quantitative, as it reports the number of pERK positive cells but does not provide any information related to their identity. Our hypothesis is that striatal pERK positive cells of both WT and AAV-Drd2KO mice are dSPNs, and that in the latter, the observed reduction in protein phosphorylation is mediated by the enhanced lateral inhibition from the D2R-depleted iSPNs. Each iSPN forms synaptic contacts with roughly one third of proximal dSPNs via GABA-ergic axon collaterals (Taverna et al., 2008) and D2R activity has been shown to suppress this lateral inhibition (Dobbs et al., 2016; Tecuapetla et al., 2009). Thus, D2R ablation will likely increase GABA release from the iSPN terminals and reduce dSPNs excitability, resulting in less dyskinesia (as reported from AAV-Drd2KO mice treated with L-DOPA) and less pERK expression.

Increase and decrease iSPN activity oppositely modulates dyskinesia

As previously discussed, several studies have addressed the causal role of D1R supersensitivity and dSPN overactivity in the generation of LID. On the contrary, the role of the indirect pathway in dyskinesia has remained largely underrated and much less investigated.

Studies on experimental models of PD and LID have demonstrated profound changes affecting iSPN intrinsic excitability and spine density in both of these pathophysiological conditions (Fieblinger et al., 2014a; Suarez et al., 2014; Zhang et al., 2013). Inspired by these seminal observations, we devoted significant efforts

at exploring how changes in iSPNs activity might contribute to modulate dyskinetic behaviours.

In Paper I, we show that iSPN stimulation inhibits the dyskinetic action of L-DOPA. Indeed, in 6-OHDA-lesioned mice G_q-DREADD activation of iSPNs markedly attenuated severity and duration of LID, even when combined with the largest and most dyskinesiogenic dose of L-DOPA (12 mg/kg).

If iSPNs activation ameliorates LID, would its inhibition have the opposite effect and aggravate dyskinesia? This was a logic question to ask considering that (i) during LID, L-DOPA decreases iSPNs activity by binding to the D2Rs (Maltese et al., 2021; Parker et al., 2018); (ii) Gs-DREADD-mediated dSPN excitation did not replicate the full severity dyskinesia observed with high doses of L-DOPA. To answer this question, we combined G_s-DREADD-dSPN stimulation with the administration of the D2R agonist quinpirole. The result of this experiment was a game changer as we could demonstrate, for the first time, that only with the simultaneous activation of dSPNs and D2R-mediated inhibition of iSPNs, we could replicate the same severity and patterns of dyskinesia only observed with very high doses of L-DOPA.

D2R role in dyskinesia and dystonia

Administration of D2R agonists to animal models of PD has led to different behavioural outcomes. Pharmacological D2R stimulation in parkinsonian rats does not appear to induce any dyskinesia (Carta et al., 2008; Lundblad et al., 2002), unless they are previously treated with L-DOPA or other D1R agonists (priming effect) (Shin et al., 2014). In contrast, treatments with selective D2R agonists in 1-methyl-4-phenyl-1,2,3,6-tetrahydropyridine (MPTP)-lesioned monkeys were reported to induce severe dyskinesia and dystonia (Boyce et al., 1990b; Gomez-Mancilla and Bedard, 1992; Luquin et al., 1992). These results overall recognize the dyskinesogenic properties of the D2R, but they do not attempt to characterize the kind of dyskinesias that result from its activation. Thus, in Paper III, our first goal was to compare different types of dyskinesias resulting from the administration of selective D1R and D2R agonists versus L-DOPA to 6-OHDA-lesioned and drug naïve mice.

Our results demonstrate that both D1R and D2R stimulation can induce dyskinetic behaviours in non-primed parkinsonian mice. Furthermore, a careful analysis of the individual AIM subtypes (axial, limb and orofacial) revealed conspicuous differences between treatments. Treatment with the selective D1R agonist SKF38393 results in rapid (‘hyperkinetic’) involuntary movements, orofacial and limb dyskinesias, whereas treatment with the selective D2R agonist sumanirole induces slow twisting movements described as severe axial dystonia. This effect was accompanied by reduced open-field mobility. Treatments acting on D2Rs, including L-DOPA, induced prolonged twisting movements and fixed abnormal postures also in other regions of the body. These features conformed to a

phenomenological definition of dystonia. As they did not fit in the classical AIMs rating scale, they were quantified with a new, *ad hoc* developed rating scale.

In human PD, dystonia is the second most common form of LID after chorea (Calabresi and Standaert, 2019) and dysfunctional signaling associated to the striatal D2Rs have been implicated in several types of dystonia (Black et al., 2014; van der Weijden et al., 2020). Likewise, studies performed in rodent and non-primate models of PD have also reported the coexistence of dystonia and hyperkinesia during treatment with L-DOPA. In the rodent models, the first proof of principle that dystonia is an important component of LID was provided by Steece-Collier and collaborators in 2003 with the development of a dystonia rating scale specific for the rat (Steece-Collier et al., 2003). Inspired by this study, Paper III presents a new dystonia scale applicable to the unilaterally lesioned mouse model. Specifically, our scale is devoted to the detection and quantification of dystonic features in dyskinesia affecting different segments of the mouse body such as trunk/neck, forelimbs, hindlimbs and tail. Two major improvements are presented in our mouse rating scale compared to the previously cited rat scale. First, the severity grades attributed to each component are anchored to precise intervals of time, making the scale more reliable. Second, our scale is not just tailored to the effect of L-DOPA but instead developed after testing a large variety of dopaminergic agonists. Thanks to the latter improvement, one of the most striking results detected by the scale was that D2R selective agonist was the only treatment capable of inducing severe hindlimb dystonia that affected both ipsilateral and contralateral sides of the body. Interestingly, also in PD patients and non-primate models of PD, “on-dystonia” are most prominent in the legs whereas hyperkinetic-choreatic features predominate in the upper part of the body (Fahn, 2000; Luquin et al., 1992).

Results from Paper III, strongly confirmed the involvement of D2Rs in complex dystonic features of dyskinesia, but left one important question still unanswered: what cell types express D2Rs that mediated these dystonic effects? We hypothesized that the answer would be the DA-denervated iSPNs. To test our hypothesis, in Paper IV we combined the 6-OHDA unilateral lesioned model to the AAV-Drd2KO mouse.

Dyskinetic and dystonic behaviors followed by treatment with the full battery of DAR agonists were compared between AAV-Drd2KO and AAV-Drd2WT control mice. Results reliably demonstrated that D2R selectively expressed in the DA-denervated iSPNs are a key factor to development of dystonia induced by L-DOPA, as their absence strongly reduced the dystonic properties of L-DOPA while maintaining its hyperkinetic components almost unaltered. Moreover, both bilateral and unilateral iSPN-D2R ablation completely prevented D2R agonist-induced dystonia.

Concluding remarks

The development of novel therapeutic approaches for movement disorders is dependent on our understanding of how the BG circuitry operates in health and disease. Historically, this question has been experimentally approached by generating lesions and/or applying pharmacological interventions to animal models, Unquestionably, these approaches have laid the foundations for many basic notions that are still valid today. However, approaches based on lesions and pharmacological stimulation have significant limitations in terms of temporal resolution and cellular specificity. Moreover, until now, the experimental investigation of movement disorders in rodent models has been limited by the use of coarse behavioural measures.

This thesis work has combined some well-established methods (such as 6-OHDA lesions and L-DOPA/DA agonist administration) with novel technologies, such as chemogenetics and gene targeting of defined cell populations. In addition, we have generated a new rating scale for the dystonic components of LID in rodents and provided novel methods to precisely track rodent motions and postures. Using this comprehensive approach, we were able to show that both hypokinetic and dyskinetic features are bidirectionally modulated by indirect- and direct BG pathways, although the relative involvement of each pathway and its corresponding DAR conditions distinct aspects of the pathological motor phenotype.

It is our hope that the new fundamental notions contributed by this thesis will pave the way for more efficient and more precise approaches to study and treat the motor abnormalities associated with PD and LID in the patients. In particular, our data lay the groundwork for a future scenario where the choice of antidyskinetic treatment will be personalised based on both the most burdensome type of involuntary movements and the regimen of dopaminergic therapies in the affected patient. Moreover, the demonstration that both hypokinetic and dyskinetic features can be potently modulated using chemogenetic pathway stimulation may raise an interest in developing similar DREADD constructs for treating the corresponding movement disorders in humans.

Acknowledgements

Acknowledgements

The journey is not made of roads, it is made of people!
This last page is dedicated to everyone who has given me support, strength, kindness and smiles during the past five years.

Angela, your passion, your attitude, and your challenges have made me the researcher I am today. Thank you!

Present and former colleagues of the Basal Ganglia Pathophysiology group:
Anki, Veronica, Irene, Francesco, Tim, Lucia, Zisis, Natalia, Lindsay, Erik, Silvia, Elena, Katrine, Chang, Morteza. I would need 100 pages more to express how important you have been to me. Instead, I will only say THANK YOU! Each one of you knows why.

Cris and *Andi*, co-supervisors and above all friends. Your passion and love for mentoring will keep inspiring future generations of young minds!

Some of my favourite smiles from BMC and outside: *Hugo*, *Vitor*, *Itzia*, *Matilde*, *Martino*, *Francesco*, *Janitha*, *Daniella*, *Andreas*, *Janko*, *Shelby*, *Per*, *Roberta*, *Marta*, *Nic*, *Sam*, *Sertan*, *Tekla*, *Iben*, *Nagesh, Susanne, Rana*. Thank you! Your smiles and kindness were daily sips of happiness!

My students, probably the biggest joy of my PhD. *Tanja*, *Joakim*, *Irene S*., *Irene R*., *Xiao*, *Sarah* and *Stefania*. Thank you, you were the real teachers!

Marcella and *Matilde*. You are the purest friendship. We grew together in this foreign land, and you will always have a special place in my (limbic system) heart!

Il viaggio non è fatto di strade ma di persone!
Quest' ultima pagina è dedicata alle persone che mi hanno dato supporto, forza, gentilezza e sorrisi durante questi cinque anni di dottorato.

Michelangelo. Tu sei il supporto, la forza, la gentilezza e i sorrisi.

Babbo, *Mamma* e *Agnese*. Famiglia significa incondizionato supporto e fiducia. Voi siete stati Famiglia in tutte le mie scelte. Grazie!

I dedicate this thesis to my *Grandparents*. The Grandparents I keep calling every Sunday, the Grandmother I lost on the way, but most of all, the Grandfather I never met and the real inspiration behind this study.

—

Questa tesi la dedico ai miei Nonni. Ai nonni che chiaccherano con me al telefono tutte le domeniche, alla nonna che ho perso da poco, ma soprattutto al nonno che non ho mai conosciuto e che piu´ di chiunque altro e´ stato d´ ispirazione a questo studio.

References

References

Albanese, A., et al., 2011. EFNS guidelines on diagnosis and treatment of primary dystonias. Eur J Neurol. 18**,** 5-18.

Albanese, A., et al., 2013. Phenomenology and classification of dystonia: a consensus update. Mov Disord. 28**,** 863-73.

Albin, R. L., et al., 1989. The functional anatomy of basal ganglia disorders. Trends Neurosci. 12**,** 366-75.

Alcacer, C., et al., 2012. Galpha(olf) mutation allows parsing the role of cAMP-dependent and extracellular signal-regulated kinase-dependent signaling in L-3,4-dihydroxyphenylalanine-induced dyskinesia. J Neurosci. 32**,** 5900-10.

Alexander, G. M., et al., 2009. Remote control of neuronal activity in transgenic mice expressing evolved G protein-coupled receptors. Neuron. 63**,** 27-39.

Aristieta, A., et al., 2021. A Disynaptic Circuit in the Globus Pallidus Controls Locomotion Inhibition. Curr Biol. 31**,** 707-721 e7.

Aristieta, A., Gittis, A., 2021. Distinct globus pallidus circuits regulate motor and cognitive functions. Trends Neurosci. 44**,** 597-599.

Armbruster, B. N., et al., 2007. Evolving the lock to fit the key to create a family of G protein-coupled receptors potently activated by an inert ligand. Proc Natl Acad Sci U S A. 104**,** 5163-8.

Assous, M., Tepper, J. M., 2019. Excitatory extrinsic afferents to striatal interneurons and interactions with striatal microcircuitry. Eur J Neurosci. 49**,** 593-603.

Aubert, I., et al., 2005. Increased D1 dopamine receptor signaling in levodopa-induced dyskinesia. Ann Neurol. 57**,** 17-26.

Bagetta, V., et al., 2012. Rebalance of striatal NMDA/AMPA receptor ratio underlies the reduced emergence of dyskinesia during D2-like dopamine agonist treatment in experimental Parkinson's disease. J Neurosci. 32**,** 17921-31.

Bamford, N. S., et al., 2004. Heterosynaptic dopamine neurotransmission selects sets of corticostriatal terminals. Neuron. 42**,** 653-63.

Bateup, H. S., et al., 2010. Distinct subclasses of medium spiny neurons differentially regulate striatal motor behaviors. Proc Natl Acad Sci U S A. 107**,** 14845-50.

Beaulieu, J. M., Gainetdinov, R. R., 2011. The physiology, signaling, and pharmacology of dopamine receptors. Pharmacol Rev. 63**,** 182-217.

Beckstead, R. M., Kersey, K. S., 1985. Immunohistochemical demonstration of differential substance P-, met-enkephalin-, and glutamic-acid-decarboxylase-containing cell body and axon distributions in the corpus striatum of the cat. J Comp Neurol. 232**,** 481-98.

Bello, E. P., et al., 2017. Inducible ablation of dopamine D2 receptors in adult mice impairs locomotion, motor skill learning and leads to severe parkinsonism. Mol Psychiatry. 22**,** 595-604.

Bernard, V., et al., 1992. Phenotypical characterization of the rat striatal neurons expressing muscarinic receptor genes. J Neurosci. 12**,** 3591-600.

Bezard, E., et al., 2001. Pathophysiology of levodopa-induced dyskinesia: potential for new therapies. Nat Rev Neurosci. 2**,** 577-88.

Bjorklund, A., Dunnett, S. B., 2007. Fifty years of dopamine research. Trends Neurosci. 30**,** 185-7.

Black, K. J., et al., 2014. Spatial reorganization of putaminal dopamine D2-like receptors in cranial and hand dystonia. PLoS One. 9**,** e88121.

Boulet, S., et al., 2006. Subthalamic stimulation-induced forelimb dyskinesias are linked to an increase in glutamate levels in the substantia nigra pars reticulata. J Neurosci. 26**,** 10768-76.

Boyce, S., et al., 1990a. Induction of chorea and dystonia in parkinsonian primates. Mov Disord. 5**,** 3-7.

Boyce, S., et al., 1990b. Differential effects of D1 and D2 agonists in MPTP-treated primates: functional implications for Parkinson's disease. Neurology. 40**,** 927-33.

Bradley, S. R., et al., 1999. Distribution of group III mGluRs in rat basal ganglia with subtype-specific antibodies. Ann N Y Acad Sci. 868**,** 531-4.

Brooks, D. J., 2006. Imaging the role of dopamine in health and disease Parkinson's disease as a lesion model. Wien Klin Wochenschr. 118**,** 570-2.

Calabresi, P., et al., 2007. Neuronal networks and synaptic plasticity in Parkinson's disease: beyond motor deficits. Parkinsonism Relat Disord. 13 Suppl 3**,** S259-62.

Calabresi, P., Standaert, D. G., 2019. Dystonia and levodopa-induced dyskinesias in Parkinson's disease: Is there a connection? Neurobiol Dis. 132**,** 104579.

Carlsson, A., et al., 1957. 3,4-Dihydroxyphenylalanine and 5-hydroxytryptophan as reserpine antagonists. Nature. 180**,** 1200.

Carta, A. R., et al., 2008. Behavioral and biochemical correlates of the dyskinetic potential of dopaminergic agonists in the 6-OHDA lesioned rat. Synapse. 62**,** 524-33.

Cazorla, M., et al., 2014. Dopamine D2 receptors regulate the anatomical and functional balance of basal ganglia circuitry. Neuron. 81**,** 153-64.

Cenci, M. A., 2014. Presynaptic Mechanisms of l-DOPA-Induced Dyskinesia: The Findings, the Debate, and the Therapeutic Implications. Front Neurol. 5**,** 242.

Cenci, M. A., et al., 1998. L-DOPA-induced dyskinesia in the rat is associated with striatal overexpression of prodynorphin- and glutamic acid decarboxylase mRNA. Eur J Neurosci. 10**,** 2694-706.

Cenci, M. A., Lundblad, M., 2007. Ratings of L-DOPA-induced dyskinesia in the unilateral 6-OHDA lesion model of Parkinson's disease in rats and mice. Curr Protoc Neurosci. Chapter 9**,** Unit 9 25.

Cenci, M. A., et al., 2011. Current options and future possibilities for the treatment of dyskinesia and motor fluctuations in Parkinson's disease. CNS Neurol Disord Drug Targets. 10**,** 670-84.

Cenci, M. A., et al., 2020. Dyskinesia matters. Mov Disord. 35**,** 392-396.

Cenci, M. A., et al., 1999. Changes in the regional and compartmental distribution of FosB- and JunB-like immunoreactivity induced in the dopamine-denervated rat striatum by acute or chronic L-dopa treatment. Neuroscience. 94**,** 515-27.

Cerri, S., Blandini, F., 2020. An update on the use of non-ergot dopamine agonists for the treatment of Parkinson's disease. Expert Opin Pharmacother. 21**,** 2279-2291.

Cersosimo, M. G., et al., 2009. Micro lesion effect of the globus pallidus internus and outcome with deep brain stimulation in patients with Parkinson disease and dystonia. Mov Disord. 24**,** 1488-93.

Chase, T. N., Oh, J. D., 2000. Striatal dopamine- and glutamate-mediated dysregulation in experimental parkinsonism. Trends Neurosci. 23**,** S86-91.

Chesselet, M. F., Graybiel, A. M., 1983. Met-enkephalin-like and dynorphin-like immunoreactivities of the basal ganglia of the cat. Life Sci. 33 Suppl 1**,** 37-40.

Corvol, J. C., et al., 2001. Galpha(olf) is necessary for coupling D1 and A2a receptors to adenylyl cyclase in the striatum. J Neurochem. 76**,** 1585-8.

Cotzias, G. C., et al., 1969. Modification of Parkinsonism--chronic treatment with L-dopa. N Engl J Med. 280**,** 337-45.

Cui, G., et al., 2013. Concurrent activation of striatal direct and indirect pathways during action initiation. Nature. 494**,** 238-42.

Cummings, J. L., 1991. Behavioral complications of drug treatment of Parkinson's disease. J Am Geriatr Soc. 39**,** 708-16.

Darmopil, S., et al., 2009. Genetic inactivation of dopamine D1 but not D2 receptors inhibits L-DOPA-induced dyskinesia and histone activation. Biol Psychiatry. 66**,** 603-13.

DeLong, M. R., 1990. Primate models of movement disorders of basal ganglia origin. Trends Neurosci. 13**,** 281-5.

Dobbs, L. K., et al., 2016. Dopamine Regulation of Lateral Inhibition between Striatal Neurons Gates the Stimulant Actions of Cocaine. Neuron. 90**,** 1100-13.

Dong, S., et al., 2010. A chemical-genetic approach for precise spatio-temporal control of cellular signaling. Mol Biosyst. 6**,** 1376-80.

Fahn, S., 1988. Concept and classification of dystonia. Adv Neurol. 50**,** 1-8.

Fahn, S., 2000. The spectrum of levodopa-induced dyskinesias. Ann Neurol. 47**,** S2-9; discussion S9-11.

Fahn, S., 2003. Description of Parkinson's disease as a clinical syndrome. Ann N Y Acad Sci. 991**,** 1-14.

Farrell, M. S., et al., 2013. A Galphas DREADD mouse for selective modulation of cAMP production in striatopallidal neurons. Neuropsychopharmacology. 38**,** 854-62.

Fearnley, J. M., Lees, A. J., 1991. Ageing and Parkinson's disease: substantia nigra regional selectivity. Brain. 114 (Pt 5)**,** 2283-301.

Fieblinger, T., et al., 2014a. Cell type-specific plasticity of striatal projection neurons in parkinsonism and L-DOPA-induced dyskinesia. Nat Commun. 5**,** 5316.

Fieblinger, T., et al., 2014b. Mechanisms of dopamine D1 receptor-mediated ERK1/2 activation in the parkinsonian striatum and their modulation by metabotropic glutamate receptor type 5. J Neurosci. 34**,** 4728-40.

Fino, E., et al., 2018. Region-specific and state-dependent action of striatal GABAergic interneurons. Nat Commun. 9**,** 3339.

Fiorentini, C., et al., 2006. Loss of synaptic D1 dopamine/N-methyl-D-aspartate glutamate receptor complexes in L-DOPA-induced dyskinesia in the rat. Mol Pharmacol. 69**,** 805-12.

Ford, C. P., 2014. The role of D2-autoreceptors in regulating dopamine neuron activity and transmission. Neuroscience. 282**,** 13-22.

Fox, S. H., et al., 2011. The Movement Disorder Society Evidence-Based Medicine Review Update: Treatments for the motor symptoms of Parkinson's disease. Mov Disord. 26 Suppl 3**,** S2-41.

Francardo, V., et al., 2011. Impact of the lesion procedure on the profiles of motor impairment and molecular responsiveness to L-DOPA in the 6-hydroxydopamine mouse model of Parkinson's disease. Neurobiol Dis. 42**,** 327-40.

Fredriksson, S., et al., 2002. Protein detection using proximity-dependent DNA ligation assays. Nat Biotechnol. 20**,** 473-7.

Gerfen, C. R., 1984. The neostriatal mosaic: compartmentalization of corticostriatal input and striatonigral output systems. Nature. 311**,** 461-4.

Gerfen, C. R., 1985. The neostriatal mosaic. I. Compartmental organization of projections from the striatum to the substantia nigra in the rat. J Comp Neurol. 236**,** 454-76.

Gerfen, C. R., 2003. D1 dopamine receptor supersensitivity in the dopamine-depleted striatum animal model of Parkinson's disease. Neuroscientist. 9**,** 455-62.

Gerfen, C. R., et al., 1990. D1 and D2 dopamine receptor-regulated gene expression of striatonigral and striatopallidal neurons. Science. 250**,** 1429-32.

Gerfen, C. R., et al., 1991. Dopamine differentially regulates dynorphin, substance P, and enkephalin expression in striatal neurons: in situ hybridization histochemical analysis. J Neurosci. 11**,** 1016-31.

Gerfen, C. R., et al., 2002. D1 dopamine receptor supersensitivity in the dopamine-depleted striatum results from a switch in the regulation of ERK1/2/MAP kinase. J Neurosci. 22**,** 5042-54.

Girasole, A. E., et al., 2018. A Subpopulation of Striatal Neurons Mediates Levodopa-Induced Dyskinesia. Neuron. 97**,** 787-795 e6.

Gittis, A. H., Kreitzer, A. C., 2012. Striatal microcircuitry and movement disorders. Trends Neurosci. 35**,** 557-64.

Gomez, J. L., et al., 2017. Chemogenetics revealed: DREADD occupancy and activation via converted clozapine. Science. 357**,** 503-507.

Gomez-Mancilla, B., Bedard, P. J., 1992. Effect of chronic treatment with (+)-PHNO, a D2 agonist in MPTP-treated monkeys. Exp Neurol. 117**,** 185-8.

Graybiel, A. M., Ragsdale, C. W., Jr., 1978. Histochemically distinct compartments in the striatum of human, monkeys, and cat demonstrated by acetylthiocholinesterase staining. Proc Natl Acad Sci U S A. 75**,** 5723-6.

Greffard, S., et al., 2006. Motor score of the Unified Parkinson Disease Rating Scale as a good predictor of Lewy body-associated neuronal loss in the substantia nigra. Arch Neurol. 63**,** 584-8.

Hersch, S. M., et al., 1994. Distribution of m1-m4 muscarinic receptor proteins in the rat striatum: light and electron microscopic immunocytochemistry using subtype-specific antibodies. J Neurosci. 14**,** 3351-63.

Herve, D., et al., 1993. G(olf) and Gs in rat basal ganglia: possible involvement of G(olf) in the coupling of dopamine D1 receptor with adenylyl cyclase. J Neurosci. 13**,** 2237-48.

Iderberg, H., et al., 2013. Modulating mGluR5 and 5-HT1A/1B receptors to treat l-DOPA-induced dyskinesia: effects of combined treatment and possible mechanisms of action. Exp Neurol. 250**,** 116-24.

Ishikawa, A., Miyatake, T., 1995. A family with hereditary juvenile dystonia-parkinsonism. Mov Disord. 10**,** 482-8.

Kawaguchi, Y., 1993. Physiological, morphological, and histochemical characterization of three classes of interneurons in rat neostriatum. J Neurosci. 13**,** 4908-23.

Kawaguchi, Y., 1997. Neostriatal cell subtypes and their functional roles. Neurosci Res. 27**,** 1-8.

Kawaguchi, Y., et al., 1995. Striatal interneurones: chemical, physiological and morphological characterization. Trends Neurosci. 18**,** 527-35.

Keifman, E., et al., 2019. Optostimulation of striatonigral terminals in substantia nigra induces dyskinesia that increases after L-DOPA in a mouse model of Parkinson's disease. Br J Pharmacol. 176**,** 2146-2161.

Kelly, M. A., et al., 2008. Role of dopamine D1-like receptors in methamphetamine locomotor responses of D2 receptor knockout mice. Genes Brain Behav. 7**,** 568-77.

Klaus, A., et al., 2017. The Spatiotemporal Organization of the Striatum Encodes Action Space. Neuron. 96**,** 949.

Klein, M. O., et al., 2019. Dopamine: Functions, Signaling, and Association with Neurological Diseases. Cell Mol Neurobiol. 39**,** 31-59.

Konradi, C., et al., 2004. Transcriptome analysis in a rat model of L-DOPA-induced dyskinesia. Neurobiol Dis. 17**,** 219-36.

Kordower, J. H., et al., 2013. Disease duration and the integrity of the nigrostriatal system in Parkinson's disease. Brain. 136**,** 2419-31.

Kravitz, A. V., et al., 2010. Regulation of parkinsonian motor behaviours by optogenetic control of basal ganglia circuitry. Nature. 466**,** 622-6.

Lebel, M., et al., 2010. Striatal inhibition of PKA prevents levodopa-induced behavioural and molecular changes in the hemiparkinsonian rat. Neurobiol Dis. 38**,** 59-67.

Lee, S. J., et al., 2021. Cell-type-specific asynchronous modulation of PKA by dopamine in learning. Nature. 590**,** 451-456.

Lemos, J. C., et al., 2016. Enhanced GABA Transmission Drives Bradykinesia Following Loss of Dopamine D2 Receptor Signaling. Neuron. 90**,** 824-38.

Lester, J., et al., 1993. Colocalization of D1 and D2 dopamine receptor mRNAs in striatal neurons. Brain Res. 621**,** 106-10.

LeWitt, P. A., et al., 1986. Dystonia in untreated parkinsonism. Clin Neuropharmacol. 9**,** 293-7.

Lowry, O. H., et al., 1951. Protein measurement with the Folin phenol reagent. J Biol Chem. 193**,** 265-75.

Lundblad, M., et al., 2002. Pharmacological validation of behavioural measures of akinesia and dyskinesia in a rat model of Parkinson's disease. Eur J Neurosci. 15**,** 120-32.

Lundblad, M., et al., 2004. A model of L-DOPA-induced dyskinesia in 6-hydroxydopamine lesioned mice: relation to motor and cellular parameters of nigrostriatal function. Neurobiol Dis. 16**,** 110-23.

Luquin, M. R., et al., 1994. Functional interaction between dopamine D1 and D2 receptors in 'MPTP' monkeys. Eur J Pharmacol. 253**,** 215-24.

Luquin, M. R., et al., 1992. Selective D2 receptor stimulation induces dyskinesia in parkinsonian monkeys. Ann Neurol. 31**,** 551-4.

Mallet, N., et al., 2012. Dichotomous organization of the external globus pallidus. Neuron. 74**,** 1075-86.

Mallet, N., et al., 2016. Arkypallidal Cells Send a Stop Signal to Striatum. Neuron. 89**,** 308-16.

Maltese, M., et al., 2021. Dopamine differentially modulates the size of projection neuron ensembles in the intact and dopamine-depleted striatum. Elife. 10.

Manson, A., et al., 2012. Levodopa-induced-dyskinesias clinical features, incidence, risk factors, management and impact on quality of life. J Parkinsons Dis. 2**,** 189-98.

Marcellino, D., et al., 2008. Identification of dopamine D1-D3 receptor heteromers. Indications for a role of synergistic D1-D3 receptor interactions in the striatum. J Biol Chem. 283**,** 26016-25.

Markowitz, J. E., et al., 2018. The Striatum Organizes 3D Behavior via Moment-to-Moment Action Selection. Cell. 174**,** 44-58 e17.

Mastro, K. J., et al., 2014. Transgenic mouse lines subdivide external segment of the globus pallidus (GPe) neurons and reveal distinct GPe output pathways. J Neurosci. 34**,** 2087-99.

Mathis, A., et al., 2018. DeepLabCut: markerless pose estimation of user-defined body parts with deep learning. Nat Neurosci. 21**,** 1281-1289.

Maurice, N., et al., 2004. D2 dopamine receptor-mediated modulation of voltage-dependent Na+ channels reduces autonomous activity in striatal cholinergic interneurons. J Neurosci. 24**,** 10289-301.

Meador-Woodruff, J. H., et al., 1991. Comparison of the distributions of D1 and D2 dopamine receptor mRNAs in rat brain. Neuropsychopharmacology. 5**,** 231-42.

Meder, D., et al., 2019. The role of dopamine in the brain - lessons learned from Parkinson's disease. Neuroimage. 190**,** 79-93.

Melamed, E., 1979. Early-morning dystonia. A late side effect of long-term levodopa therapy in Parkinson's disease. Arch Neurol. 36**,** 308-10.

Metman, L. V., et al., 1999. Amantadine for levodopa-induced dyskinesias: a 1-year follow-up study. Arch Neurol. 56**,** 1383-6.

Morelli, M., et al., 1989. Time and dose dependence of the 'priming' of the expression of dopamine receptor supersensitivity. Eur J Pharmacol. 162**,** 329-35.

Morin, N., et al., 2013. MPEP, an mGlu5 receptor antagonist, reduces the development of L-DOPA-induced motor complications in de novo parkinsonian monkeys: biochemical correlates. Neuropharmacology. 66**,** 355-64.

Muller, T., Russ, H., 2006. Levodopa, motor fluctuations and dyskinesia in Parkinson's disease. Expert Opin Pharmacother. 7**,** 1715-30.

Munoz-Manchado, A. B., et al., 2018. Diversity of Interneurons in the Dorsal Striatum Revealed by Single-Cell RNA Sequencing and PatchSeq. Cell Rep. 24**,** 2179-2190 e7.

Nakajima, K., Wess, J., 2012. Design and functional characterization of a novel, arrestin-biased designer G protein-coupled receptor. Mol Pharmacol. 82**,** 575-82.

Nelson, A. B., Kreitzer, A. C., 2014. Reassessing models of basal ganglia function and dysfunction. Annu Rev Neurosci. 37**,** 117-35.

Novak, M., et al., 2010. Incentive learning underlying cocaine-seeking requires mGluR5 receptors located on dopamine D1 receptor-expressing neurons. J Neurosci. 30**,** 11973-82.

Oh, J. D., et al., 1997. Protein kinase A inhibitor attenuates levodopa-induced motor response alterations in the hemi-parkinsonian rat. Neurosci Lett. 228**,** 5-8.

Olanow, C. W., et al., 2020. Once-Weekly Subcutaneous Delivery of Polymer-Linked Rotigotine (SER-214) Provides Continuous Plasma Levels in Parkinson's Disease Patients. Mov Disord. 35**,** 1055-1061.

Ouattara, B., et al., 2011. Metabotropic glutamate receptor type 5 in levodopa-induced motor complications. Neurobiol Aging. 32**,** 1286-95.

Parker, J. G., et al., 2018. Diametric neural ensemble dynamics in parkinsonian and dyskinetic states. Nature. 557**,** 177-182.

Parkinson, J., 2002. An essay on the shaking palsy. 1817. J Neuropsychiatry Clin Neurosci. 14**,** 223-36; discussion 222.

Pavon, N., et al., 2006. ERK phosphorylation and FosB expression are associated with L-DOPA-induced dyskinesia in hemiparkinsonian mice. Biol Psychiatry. 59**,** 64-74.

Pin, J. P., Acher, F., 2002. The metabotropic glutamate receptors: structure, activation mechanism and pharmacology. Curr Drug Targets CNS Neurol Disord. 1**,** 297-317.

Redgrave, P., et al., 1999. The basal ganglia: a vertebrate solution to the selection problem? Neuroscience. 89**,** 1009-23.

Redgrave, P., et al., 2010. Goal-directed and habitual control in the basal ganglia: implications for Parkinson's disease. Nat Rev Neurosci. 11**,** 760-72.

Ridray, S., et al., 1998. Coexpression of dopamine D1 and D3 receptors in islands of Calleja and shell of nucleus accumbens of the rat: opposite and synergistic functional interactions. Eur J Neurosci. 10**,** 1676-86.

Rivera, A., et al., 2002a. Molecular phenotype of rat striatal neurons expressing the dopamine D5 receptor subtype. Eur J Neurosci. 16**,** 2049-58.

Rivera, A., et al., 2002b. Dopamine D4 receptors are heterogeneously distributed in the striosomes/matrix compartments of the striatum. J Neurochem. 80**,** 219-29.

Robelet, S., et al., 2004. Chronic L-DOPA treatment increases extracellular glutamate levels and GLT1 expression in the basal ganglia in a rat model of Parkinson's disease. Eur J Neurosci. 20**,** 1255-66.

Rogan, S. C., Roth, B. L., 2011. Remote control of neuronal signaling. Pharmacol Rev. 63**,** 291-315.

Roth, B. L., 2016. DREADDs for Neuroscientists. Neuron. 89**,** 683-94.

Royo-Villanova, C., et al., 2001. [Neisseria meningitidis pneumoniae in a 47 year old woman with systemic lupus]. Enferm Infecc Microbiol Clin. 19**,** 188-9.

Ryan, M. B., et al., 2018. Aberrant Striatal Activity in Parkinsonism and Levodopa-Induced Dyskinesia. Cell Rep. 23**,** 3438-3446 e5.

Rylander, D., et al., 2010. A mGluR5 antagonist under clinical development improves L-DOPA-induced dyskinesia in parkinsonian rats and monkeys. Neurobiol Dis. 39**,** 352-61.

Rylander, D., et al., 2009. Pharmacological modulation of glutamate transmission in a rat model of L-DOPA-induced dyskinesia: effects on motor behavior and striatal nuclear signaling. J Pharmacol Exp Ther. 330**,** 227-35.

Santini, E., et al., 2009. L-DOPA activates ERK signaling and phosphorylates histone H3 in the striatonigral medium spiny neurons of hemiparkinsonian mice. J Neurochem. 108**,** 621-33.

Santini, E., et al., 2012. Dopamine- and cAMP-regulated phosphoprotein of 32-kDa (DARPP-32)-dependent activation of extracellular signal-regulated kinase (ERK) and mammalian target of rapamycin complex 1 (mTORC1) signaling in experimental parkinsonism. J Biol Chem. 287**,** 27806-12.

Santini, E., et al., 2007. Critical involvement of cAMP/DARPP-32 and extracellular signal-regulated protein kinase signaling in L-DOPA-induced dyskinesia. J Neurosci. 27**,** 6995-7005.

Schindelin, J., et al., 2012. Fiji: an open-source platform for biological-image analysis. Nat Methods. 9**,** 676-82.

Sebastianutto, I., Cenci, M. A., 2018. mGlu receptors in the treatment of Parkinson's disease and L-DOPA-induced dyskinesia. Curr Opin Pharmacol. 38**,** 81-89.

Sebastianutto, I., et al., 2020. D1-mGlu5 heteromers mediate noncanonical dopamine signaling in Parkinson's disease. J Clin Invest.

Sgambato-Faure, V., Cenci, M. A., 2012. Glutamatergic mechanisms in the dyskinesias induced by pharmacological dopamine replacement and deep brain stimulation for the treatment of Parkinson's disease. Prog Neurobiol. 96**,** 69-86.

Shen, W., et al., 2008. Dichotomous dopaminergic control of striatal synaptic plasticity. Science. 321**,** 848-51.
Shetty, A. S., et al., 2019. Dystonia and Parkinson's disease: What is the relationship? Neurobiol Dis. 132**,** 104462.
Shin, E., et al., 2014. The anti-dyskinetic effect of dopamine receptor blockade is enhanced in parkinsonian rats following dopamine neuron transplantation. Neurobiol Dis. 62**,** 233-40.
Shuen, J. A., et al., 2008. Drd1a-tdTomato BAC transgenic mice for simultaneous visualization of medium spiny neurons in the direct and indirect pathways of the basal ganglia. J Neurosci. 28**,** 2681-5.
Sibley, D. R., Monsma, F. J., Jr., 1992. Molecular biology of dopamine receptors. Trends Pharmacol Sci. 13**,** 61-9.
Sibley, D. R., et al., 1992. Molecular neurobiology of dopamine receptor subtypes. Neurochem Int. 20 Suppl**,** 17S-22S.
Smith, Y., Kieval, J. Z., 2000. Anatomy of the dopamine system in the basal ganglia. Trends Neurosci. 23**,** S28-33.
Smith, Y., et al., 2004. The thalamostriatal system: a highly specific network of the basal ganglia circuitry. Trends Neurosci. 27**,** 520-7.
Snyder, G. L., et al., 2000. Regulation of phosphorylation of the GluR1 AMPA receptor in the neostriatum by dopamine and psychostimulants in vivo. J Neurosci. 20**,** 4480-8.
St-Hilaire, M., et al., 2005. Denervation and repeated L-DOPA induce complex regulatory changes in neurochemical phenotypes of striatal neurons: implication of a dopamine D1-dependent mechanism. Neurobiol Dis. 20**,** 450-60.
Steece-Collier, K., et al., 2003. Embryonic mesencephalic grafts increase levodopa-induced forelimb hyperkinesia in parkinsonian rats. Mov Disord. 18**,** 1442-54.
Suarez, L. M., et al., 2014. L-DOPA treatment selectively restores spine density in dopamine receptor D2-expressing projection neurons in dyskinetic mice. Biol Psychiatry. 75**,** 711-22.
Sulzer, D., 2007. Multiple hit hypotheses for dopamine neuron loss in Parkinson's disease. Trends Neurosci. 30**,** 244-50.
Surmeier, D. J., et al., 1992. Dopamine receptor subtypes colocalize in rat striatonigral neurons. Proc Natl Acad Sci U S A. 89**,** 10178-82.
Surmeier, D. J., et al., 1996. Coordinated expression of dopamine receptors in neostriatal medium spiny neurons. J Neurosci. 16**,** 6579-91.
Tauscher, J., et al., 2004. Equivalent occupancy of dopamine D1 and D2 receptors with clozapine: differentiation from other atypical antipsychotics. Am J Psychiatry. 161**,** 1620-5.
Taverna, S., et al., 2008. Recurrent collateral connections of striatal medium spiny neurons are disrupted in models of Parkinson's disease. J Neurosci. 28**,** 5504-12.
Tecuapetla, F., et al., 2009. Differential dopaminergic modulation of neostriatal synaptic connections of striatopallidal axon collaterals. J Neurosci. 29**,** 8977-90.
Tecuapetla, F., et al., 2014. Balanced activity in basal ganglia projection pathways is critical for contraversive movements. Nat Commun. 5**,** 4315.
Tepper, J. M., et al., 2004. GABAergic microcircuits in the neostriatum. Trends Neurosci. 27**,** 662-9.
Thanvi, B., et al., 2007. Levodopa-induced dyskinesia in Parkinson's disease: clinical features, pathogenesis, prevention and treatment. Postgrad Med J. 83**,** 384-8.
Valjent, E., et al., 2009. Looking BAC at striatal signaling: cell-specific analysis in new transgenic mice. Trends Neurosci. 32**,** 538-47.

van der Weijden, M. C. M., et al., 2020. A Gain-of-Function Variant in Dopamine D2 Receptor and Progressive Chorea and Dystonia Phenotype. Mov Disord.

Vardy, E., et al., 2015. A New DREADD Facilitates the Multiplexed Chemogenetic Interrogation of Behavior. Neuron. 86**,** 936-946.

Vargas, A. P., et al., 2019. Impulse control symptoms in patients with Parkinson's disease: The influence of dopaminergic agonist. Parkinsonism Relat Disord. 68**,** 17-21.

Voon, V., et al., 2017. Impulse control disorders and levodopa-induced dyskinesias in Parkinson's disease: an update. Lancet Neurol. 16**,** 238-250.

Westin, J. E., et al., 2001. Persistent changes in striatal gene expression induced by long-term L-DOPA treatment in a rat model of Parkinson's disease. Eur J Neurosci. 14**,** 1171-6.

Westin, J. E., et al., 2007. Spatiotemporal pattern of striatal ERK1/2 phosphorylation in a rat model of L-DOPA-induced dyskinesia and the role of dopamine D1 receptors. Biol Psychiatry. 62**,** 800-10.

Xu, J., et al., 2009. mGluR5 has a critical role in inhibitory learning. J Neurosci. 29**,** 3676-84.

Zauber, S. E., et al., 2009. Stimulation-induced parkinsonism after posteroventral deep brain stimulation of the globus pallidus internus for craniocervical dystonia. J Neurosurg. 110**,** 229-33.

Zhang, Y., et al., 2013. Aberrant restoration of spines and their synapses in L-DOPA-induced dyskinesia: involvement of corticostriatal but not thalamostriatal synapses. J Neurosci. 33**,** 11655-67.